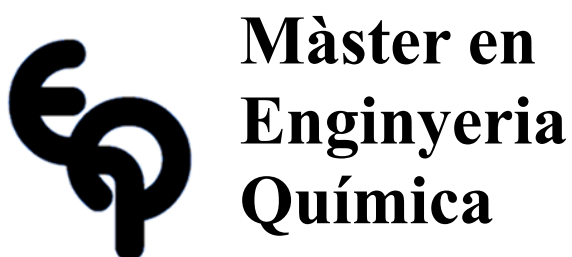


Tutor/s

Dr. Jordi H. Badia i Córcoles
*Chemical Engineering and Analytical
Chemistry Department*

Dra. Eliana Ramírez Rangel
*Chemical Engineering and Analytical
Chemistry Department*



Treball Final de Màster

Bifunctional catalyst synthesis using ion-exchange resins for the methyl isobutyl ketone production

Síntesi de catalitzadors bifuncionals emprant resines de bescanvi iònic per a la producció de metil-isobutil cetona

Eloi Canadell I Soler

February 2023



UNIVERSITAT DE
BARCELONA

Dos campus d'excel·lència internacional

B:KC Barcelona
Knowledge
Campus

HUB^c Health Universitat
de Barcelona
Campus

Aquesta obra esta subjecta a la llicència de
Reconeixement-NoComercial-SenseObraDerivada



<http://creativecommons.org/licenses/by-nc-nd/3.0/es/>

Després d'un fracàs, els plans més elaborats semblen absurds

Fiódor Dostoyevski

Primer de tot m'agradaria dedicar unes paraules d'agraïment als tutors d'aquest projecte, Dr. Jordi Hug Badia i Dra. Eliana Ramírez, per la confiança i la oportunitat de realitzar-lo, així com l'ajuda que se m'ha proporcionat durant el transcurs del mateix. També, m'agradaria agrair al Dr. Rodrigo Soto el temps dedicat a la caracterització de catalitzadors ja que ha sigut de gran ajuda. Seguidament, vull donar les gràcies a cada membre del grup de recerca de cinètica aplicada i catàlisi ja que d'una manera o una altre, han incidit en el resultat final d'aquest projecte.

En segon lloc, crec que és necessari agrair als amics, de dins i de fora del màster, per ser al costat meu durant els moments més foscos.

Finalment, he de donar les gràcies a la meva família ja que des de ben petit, ha sigut el meu suport incondicional. M'han sabut aconsellar i animar, i el que és més important, que a través dels seus esforços s'ha forjat la persona que sóc avui en dia. Una especial menció a la Noelia, que és la persona que més ha patit la meva absència per estar dedicant temps al treball, la persona que ha aguantat els canvis d'humors constants i la persona que sempre ha estat al meu costat.

REPORT

CONTENTS

SUMMARY	i
SUSTAINABLE DEVELOPMENT GOALS	ii
1. Introduction.....	1
1.1. Biomass.....	1
1.2. Acetone.....	2
1.2.1. Methyl Isobutyl Ketone	3
1.3. Catalysis	3
1.3.1. Ion exchange resins	5
1.4. State of the art.....	6
2. Objectives	8
3. Formulas for the calculation of the different parameters	9
4. Experimental section	10
4.1. Materials.....	10
4.2. Catalyst preparation protocol and characterization	11
4.3. Setup.....	13
4.4. Catalytic activity test procedure.....	14
4.5. Reaction conditions	15
5. Results and discussion	16
5.1. Calibration	16
5.2. Catalytic activity test	17
5.3. Catalyst characterization	19
5.4. Catalytic activity test at different operating temperatures	27
5.5. Catalyst reuse	28
6. Conclusions and future work.....	32
7. References	34

Acronyms	39
Appendices	40
Appendix 1: Determination of the acid capacity.....	40
Appendix 2: Chromatographic response	41
Appendix 3: Graphical representation of the calibration equations	42
Appendix 4: TEM images of the tested catalysts	44
Appendix 5: Metal size distributions of the tested catalysts	48
Appendix 6: SEM images of the prepared catalysts	50

SUMMARY

This project is focused on the preparation of bifunctional catalysts, using ion exchange resins as a supporting material, for the biomass transformation. The acetone hydrogenation to produce methyl isobutyl ketone (MIBK), under the one-pot synthesis approach was selected as a model reaction.

Acidic ion exchange resins, Amberlyst™ 15 (A15) and Dowex 50WX2 (Dow2), were selected as the supporting material due to their ability to carry out the reactions at milder conditions. These resins were doped with noble metals (Pd and Ru) and non-noble metals (Cu) by wet impregnation.

The catalytic activity test consisted on hydrogenating 40 g of acetone with a 5 wt.% catalyst loading for 4 h at 120 °C, a hydrogen pressure of 30 barg at 300 rpm. Palladium doped resins resulted to be the more catalytically active being able to convert more than 30 % of the acetone being totally selective to the MIBK formation. Similar results were accomplished by a commercial catalyst, namely Amberlyst™ CH28 (ACH28). Although Dow2 doped with 1 wt.% achieved the highest yield, 37 %, it was less catalytically active than ACH28 according to the turnover number which were, respectively, 1500 and 1839 mols of acetone converted per mole of metal supported on the catalyst. Cu-based catalyst resulted to be the least catalytically active converting less than 20 % of the acetone with a selectivity towards the product of interest inferior to 10 %.

Cu- and Pd-catalysts were characterized. It was observed that the nominal and actual metal content were seen to match at 1 wt.%. Additionally, no acidic sites were lost during the catalytic test, although the Pd-catalyst lost some acidic sites during its preparation. The transmission electron microscope proved that the Dow2-1%Pd catalyst had the smallest size distribution, which makes it a great catalyst while the scanning electron microscopy proved that the metal was homogeneously distributed on the polymeric resin surface.

Finally, the Dow2-1%Pd catalyst was assayed at different temperatures (110-130 °C), being able to convert 45 % of the initial acetone without a selectivity loss. However, its reusability is not feasible, although the TON number remains constant, because almost no production of MIBK was observed when tested in three consecutive experimental runs.

Keywords: Biomass, bifunctional catalysts, catalytic study, ion exchange resins.

SUSTAINABLE DEVELOPMENT GOALS

Sustainability can be defined as the fulfillment of the current generation needs without comprising the needs of future generations while ensuring a balance between the three pillars: economic growth, social well-being, and environmental protection.

Lately, society has become more interested in sustainability to protect somehow the environment. Therefore, all the innovations that are taking place are trying to be related to at least one of the seventeen categories of the UN Sustainable Development which are shown in the next image.



This project will most likely make an impact on the 13th category of the sustainable development goals, the climate action. It is thought so because the bifunctional catalysts are prepared to carry out biomass transformation reactions under the one-pot synthesis approach under milder conditions. In other words, with these catalysts many petrol-based products could be substituted by products of renewable sources, therefore carbon dioxide emissions could be reduced. The fact, that these catalysts aim to carry out the reaction under the one-pot synthesis approach and milder conditions, have a direct impact on the efficiency of the reaction since less utilities are required which also means an increasement of the safety since the operating conditions are less extreme.

In conclusion, this project can be aligned to the sustainable development goals since it is related to at least two different categories. Furthermore, these catalysts could be tested in different reactions giving the project an opportunity to have an impact in other categories, such as the 7th category because from biomass transformation reactions, many products can be synthesized to end up obtaining energy.

1. INTRODUCTION

Fossil resources are hydrocarbon-containing materials formed as a result of different transformations acting on the remains of organic matter over periods of millions of years. Nowadays, our society has a great dependence on fossil resources because 86 % of the energy and 96 % of the organic chemicals are obtained from these resources [1].

Unfortunately, fossil resources present two major concerns, namely its depletion, since they are not renewed in a time period relevant to the resource consumption and the environmental concern they raise, due to the greenhouse gases emissions caused by the excessive reliance on this kind of resources [1,2].

Due to these concerns, the research for renewable alternatives has increased significantly trying to transition from fossil-fuels to renewable resources for chemicals, fuels and materials production [3–5]. Biomass has drawn certain attention since it is a source of renewable organic carbon that can be converted to value-added chemicals, liquid fuels or functional materials [2,4].

1.1. BIOMASS

From a biorefinery perspective, biomass could refer to all the organic material that could be potentially converted into fuels and chemicals [5]. In fact, biomass sources could be divided into different generations [5]:

- First generation: biomass obtained from food crops.
- Second generation: non-edible plant residues, such as agricultural wastes.
- Third generation: biomass obtained from algae.

At the moment, the most feasible generation to produce renewable-alternatives to petrol-based products is the second generation of biomass sources, because the first generation must compete with food crops while the third generation suffers from a lack of development [5,6].

In the second generation, the most abundant source of biomass are the lignocellulosic materials [6]. These are composed by:

- Hemicellulose: It is an amorphous short-chain polymer made of glucose and xylose [5,7].

- Lignin: It is a hydrophobic aromatic polymer, highly cross-linked, that provides structural rigidity to plants [5,8].
- Cellulose: Linear and crystalline homopolymer formed as a result of the glucose polymerization [5,8].

The sugars contained in these materials can be transformed into bioproducts by fermentation or chemical transformation [8]. Acetone, butanol, ethanol, lactic acid, acetate, and succinate, among other products, can be produced through biomass fermentation [9,10]. With the chemical transformation of the sugars contained in biomass, many platform chemicals, which are molecules from which a wide range of products are produced, can be synthesized, such as levulinic acid, furfural or hydroxymethyl furfural, among others [11]. Even though the above-mentioned compounds have been produced through different approaches, their upgrading to value-added chemicals usually require catalytic reaction processes [11].

1.2. ACETONE

While being the simplest example of ketones, acetone is the most widely used ketone in industry [12]. It is a colorless liquid that is completely miscible with water and most organic solvents and oils [12]. Therefore, it is considered an important solvent in the industry, a common building block in organic chemistry, and a precursor to polymers, besides the domestic uses, as a nail polish remover and paint thinner [12].

Nowadays, most of the acetone is obtained as a phenol byproduct using the cumene process [13,14]. In fact, around 90 % of the US acetone was produced through this process in 2011 [14]. Even though the great majority of the acetone is synthesized from fossil resources, there are alternative routes to produce this compound. Acetone can be produced by greener way through the acetone-butanol-ethanol (ABE) fermentation process which was developed in the first half of the 20th century to produce acetone for military applications [5,13]. With this process acetone, butanol and ethanol are produced in the mass ratio of 3:6:1 respectively [5,13]. These compounds are produced via fermentation, under anaerobic conditions, with a strain of microorganisms called *Clostridium* that can digest sugars, starch, cellulose and lignin [5,15]. Therefore, acetone can be produced from first and second generation biomass sources [15].

The ABE fermentation consists on a two-phase process which includes the acidogenic phase and the solventogenic phase [5]. During the acidogenic phase, the bacteria and production of acetate and butyrate takes place while in the solventogenic the growth stops and the metabolism changes, where the acidogenic products are re-assimilated and converted to the products of interest, namely acetone, butanol and ethanol [15].

Many value-added chemicals can be produced from acetone such as solvents, methyl methacrylate, bisphenol A, or pharmaceutical products [16].

1.2.1. Methyl Isobutyl Ketone

Methyl isobutyl ketone (MIBK) or 4-methylpentan-2-one is a chemical compound that is mainly used as a solvent, for paints or coatings, extracting medium, in the synthesis of antibiotics and lubricants, intermediate in the production of epoxy, or as a flavoring agent [17].

This acetone derivative is produced through a three-steps reaction process which involves an acidic aldol condensation of the acetone to produce diacetone alcohol (DAA), an acid-catalyzed dehydration of the DAA to obtain mesityl oxide (MO), and, finally, the metal-catalyzed hydrogenation to produce the compound of interest, MIBK [17,18]. A scheme of the global reaction pathway is shown in Figure 1.

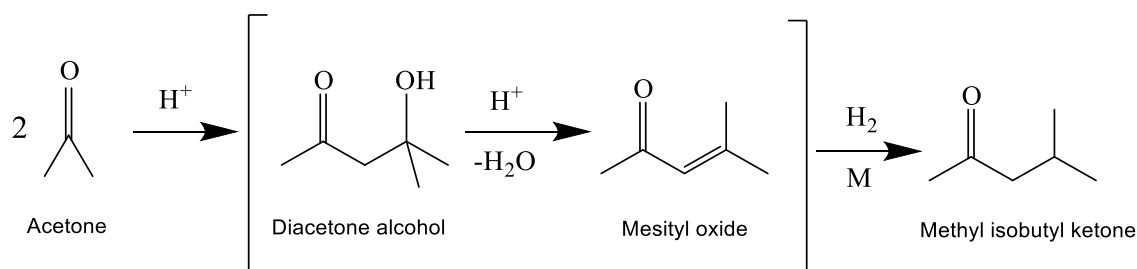


Figure 1. MIBK reaction pathway

Traditionally, this reaction was carried out through homogeneous catalysis which caused pollution and corrosion problems [19]. Nowadays, due to these problems, the reaction is being carried out on heterogeneous multifunctional catalysts, which also allows to carry out the reaction under a one-pot synthesis approach [19,20].

1.3. CATALYSIS

A catalyst can be defined as a substance that increases the rate at which a chemical reaction occurs without permanently intervening in it [21]. The catalyzed reactions can be classified into three different groups [21]:

- 1) Homogeneous, where the catalyst is found in the same phase as the reactants.
- 2) Heterogeneous, where the catalyst and reactants are in different phases.
- 3) Enzymatic, where an enzyme acts as a catalyst.

Catalysis plays an important role in the current efforts to achieve more sustainable chemical processes by means of process intensification [22]. Intensification consists in replacing chemical processes that included several reaction steps with intermediate product separation and purification by one-pot synthesis approach [22]. Among the one-pot multistep reactions, those catalyzed by transition metals play an important role in synthetic chemistry, mainly due to the diversity of the available transformations [23].

Regardless the class of reaction, mono- or multi-multisite, the great majority of the procedures usually require homogeneous metallic complexes [23]. Even though homogeneous catalysts are exceptionally efficient, they present different concerns such as the product contamination, catalyst separation or corrosion-derived problems [23,24]. In fact, nowadays, only 20 % of the chemical reactions are currently based on homogeneous catalysis [21].

Heterogeneous catalysts are promising candidates to overcome some of the problems with the homogeneous catalysts [22,23]. This kind of catalysts presents certain advantages, such as the easy separation from the products, possible reuse of the catalyst or recycle of the same in another reaction, and, if it contains metal sites, it reduces the chance of product contamination [22,23]. Additionally, heterogeneous catalysts allow generating robust, well-defined and multisite materials in which active sites can act both cooperatively or independently in a given cascade process [22].

A heterogeneous bifunctional catalyst could be then defined as a multisite solid catalyst. A typical cascade process carried out on a heterogeneous catalysts could be the aldol condensation followed by dehydration and hydrogenation, which is the case of the MIBK synthesis [22].

A typical bifunctional heterogeneous catalyst consists of the following parts [21]:

- Active component: Responsible for increasing the reaction rate. Many different substances can be used as an active component depending on the type of reaction. On one hand for the redox reaction transition metals, transition metals oxides or transition metals sulfides will most likely be used. On the other hand,

for reactions with formation of carbon ions, solid acids and functionalized polymers will be used.

- Support: It is a material with a high surface area, that favors the dispersion of the active component, as well as its stabilization it. Some commercial supports are aluminum oxide, silica, zeolites or activated carbon.

1.3.1. Ion exchange resins

From a catalytic point of view, ion exchange resins are polymeric catalysts [25]. These are solid organic materials with hydrophilic functional groups anchored on a polymeric matrix of hydrophobic nature [25–27]. The so-called matrix is constructed from linear polymeric chains, cross-linked with each other. Usually this matrix is made of polystyrene cross-linked with divinylbenzene [26–28]. Actually, one of the most common ion exchange resin is sulphonated polystyrene cross-linked with divinylbenzene [26,28].

From a morphological point of view, two different commercial types of resins can be distinguished: gel-type and macroreticular [29,30]. On one side, gel-type resins, also known as microporous resins, lack of appreciable porous in dry state and its interior is only accessible after swelling [29]. On the other side macroreticular resins, also known as macroporous resins, possess stable pores in dry state, in addition to those generated by the swelling of the polymer skeleton [29]. These two types of resins are also distinguished by the crosslinking degree, since the gel-type resins are low-crosslinked solids (1-8 % DVB), the macroreticular resins usually have a higher cross link degree (5-60 % DVB) [26].

When selecting an ion exchange resin, there are some parameters that need to be taken into account such as [26,28,30]:

- Ion exchange capacity: It corresponds to the number of functional groups, available for any kind of ion exchange, per gram of dry resin. Thus, in the case of cationic resins, it is expressed as meqH⁺/g.
- Crosslinking degree: It is referred to the content of the crosslinking agent in polymeric chains of the resin. Therefore, it is usually expressed as the weight percentage of divinylbenzene.

- Porosity: It corresponds to the cavities that remain in the polymer matrix. Usually, the more porous a resin is, the lesser is the crosslinking degree.
- Specific area: It is referred to the total surface, outer and pores, per mass unit of the dried ion exchange resin.
- Swelling degree: When an ion exchange resin is in contact with a polar solvent, it usually undergoes a structural change compared to the dry state due to the swelling.
- Density: Weight of dry resin per unit of volume of the ion exchange resin.
- Stability: In a certain way, it is a property that guarantees the operability of the catalyst at long-term.

Usually, the ion exchange resins are supplied in spherical beads in the range of 0.3-1.25 mm [29].

1.4. STATE OF THE ART

For the MIBK manufacturing, two different catalysts are available: polymeric and inorganic catalysts [20]. But polymeric catalysts present a major advantage compared to inorganic catalysts, which is the possibility to achieve high yields and selectivity under milder conditions and, consequently, being able to carry out the process intensification under milder conditions [20]. In fact, a commercial polymeric acidic catalyst doped with palladium, AmberlystTM CH28 (ACH28), has been successfully tested in both batch and continuous conditions [20].

Several works in the literature have reported the use of inorganic supporting materials, such as zeolites or silicas, doped with metals such as Pd, Ni or Cu [18,20]. In Table 1, literature references related to MIBK synthesis in a batch reactor under a one-pot synthesis approach and relatively mild conditions are presented.

Table 1. State of the art

	S. Talwalkar 2006 [18]	J.A. Trejo 2010 [20]	F. Liguori 2021 [17]	Y. Higashio 1996 [31]	Y.Z. Chen 2001 [32]	R.D. Hetterley 2006 [33]	E. Kozhevnikova 2006 [34]	F. Al-Wadaani 2008 [35]
m_{acetone}[g]	100	2.77	4.71	50	50	2	2	2
Solvent (wt.%)	-	-	-	-	-	Decane (13 %)	Decane (13 %)	Decane (13 %)
Catalyst	ACH28	ACH28	0.26PD@X- link-08-PW79	0.1%Pd -Niobic acid	0.1%Pd- Niobia (3) on silica	0.1%Pd/CsPW	1%Pd/Zn- Cr(1:10)	0.3%Pd/Zn- Cr(1:30)
Catalyst load [wt./wt. of acetone]	5.0	36.1	2.1	4.0	0.8	10.0	10.0	10.0
T [°C]	120	110	140	160	160	180	200	180
P_{H2} [bar]	30	14	10	19.61	20	7.5	5	7.5
t [h]	3.5	4	4	2	2	2	2	2
X_{acetone} [%]	45.0	66.0	19.7	45.6	17.7	42.1	55.6	55.8
S_{MIBK} [%]	96.5	94.0	91.0	92.5	91.5	89.8	83.1	66.5
Y_{MIBK} [%]	43.4	62.0	17.9	42.2	16.2	37.8	46.2	37.1

2. OBJECTIVES

The present work focuses on the synthesis of bifunctional catalyst from commercial ion exchange resins as the supporting material. The prepared catalysts will be tested for the MIBK synthesis in a batch reactor under a one-pot synthesis approach and moderate conditions. Therefore, the specific goals of the project are:

- 1) Synthesis of bifunctional catalysts, by ion-exchange in aqueous media, using commercial ion exchange resins as the supporting materials and doping them with noble (Pd and Ru) and non-noble metals (Cu).
- 2) Characterization of the different catalysts with the following techniques: Inductively coupled plasma mass spectrometry (ICP-MS), X-ray diffraction (XRD), Transmission electron microscopy (TEM), Scanning electron microscopy (SEM), Brunauer-Emmett-Teller adsorption method, and determination of the acid capacity by volumetric titration against a standard base.
- 3) Performance comparison between the prepared catalysts and the commercial bifunctional catalyst (ACH28) in the MIBK synthesis under mild conditions in a one-pot synthesis approach. Selection of the best catalyst in terms of yield towards MIBK.
- 4) Study the behavior of the best catalyst when performing at different temperatures.
- 5) Reusability evaluation of the best catalyst in the synthesis of the MIBK under a one-pot synthesis approach with three consecutive experimental runs.

3. CALCULATIONS

Acetone conversion, expressed as a percentage, was calculated as shown in Equation 1:

$$X_{Ac} = \frac{n_{Ac,0} - n_{Ac,f}}{n_{Ac,0}} \cdot 100 \quad (1)$$

where $n_{Ac,0}$ stands for the initial moles of acetone and $n_{Ac,f}$ corresponds to the final moles of acetone.

Selectivity, expressed as a percentage, towards MIBK was calculated as follows:

$$S_{MIBK} = \frac{2 \cdot n_{MIBK}}{n_{Ac,0} - n_{Ac,f}} \cdot 100 \quad (2)$$

where n_{MIBK} is the moles of MIBK.

The yield towards MIBK, expressed as a percentage, can be calculated as:

$$Y_{MIBK} = \frac{X_{Ac} \cdot S_{MIBK}}{100} \quad (3)$$

The turnover number (TON) is defined as a the number of substrate moles that a single mol of catalyst can convert before its deactivation [36]. Therefore, it is a parameter that evaluates the catalytic activity. In the present work, TON is referred to the active metal sites, and it has been calculated with the following expression:

$$TON = \frac{n_{Ac,0} - n_{Ac,f}}{n_M} \quad (4)$$

where n_M corresponds to the metal mols in the catalyst.

4. EXPERIMENTAL SECTION

4.1. MATERIALS

In the present work, commercial ion exchange resins were doped to obtain bifunctional catalysts. For their preparation, the commercial acidic ion exchange resins Amberlyst™ 15 (A15) and Dowex 50Wx2 100-200 mesh (Dow2) were used as supporting materials. These catalysts were supplied by DuPont and Across Organics, respectively, and their main properties are shown in Table 2. In addition, this project meant to compare the prepared catalysts to the commercial bifunctional catalyst Amberlyst™ CH28 (ACH28), also included in Table 2, which presents a nominal palladium amount of 0.7 wt.% on dry basis.

Table 2. Catalyst properties according to the suppliers.

Catalyst	Type	Sulfonation	Acid Capacity [meqH ⁺ /g]	DVB [%]	Water retention [%]	T _{max} [°C]	ρ [g/cm ³]
A15 [37]	Macro	Conventional	4.81	20	52-57	120	1.416
Dow2 [38]	Micro	Conventional	4.98	2	74-82	150	0.74
ACH28 [39]	Macro	Conventional	4.80	N/A	52-58	130	0.790

The precursor salts that have been used to dope the different commercial ion exchange resins, along with their properties are shown in Table 3.

Table 3. Precursor salt main characteristics.

Precursor Salt	Mw [g/mol]	Purity [wt.%]	Supplier	Hazards
Pd(NH₃)₄Cl₂·H₂O	263.46	99.9	Alfa Aesar	
RuCl₃, anhydrous	207.43	47.7	Alfa Aesar	
CuCl₂·2H₂O	170.48	98.5	PanReac	

In the present work, the MIBK synthesis from acetone in a multistep process has been studied without the presence of a solvent. A calibration of the system, with high purity components, was required to identify and quantify the detected species in the product

mixture. Thus, acetone, water, MO, and MIBK were required. Their main properties can be found in Table 4.

Table 4. Main properties of the reactants and calibration species

Properties	Acetone [40]	Hydrogen [41]	Water [42]	MO [43]	MIBK [44]
CAS number	67-64-1	1333-74-0	7732-18-5	141-79-7	108-10-1
Molecular formula	C ₃ H ₆ O	H ₂	H ₂ O	C ₆ H ₁₀ O	C ₆ H ₁₂ O
Molecular weight [g/mol]	58.08	2	18	98.14	100.16
Purity [wt.%]	99.5	99.999	100	99	98.5
Density [g/cm³]	0.787 – 0.791 at 20/4	0.089	0.998	0.854	0.800
Melting point [°C]	-94	-259.2	0	-53	-85
Boiling point [°C]	56.5	-252.9	100	129	116.5
Flash point at 1 atm [°C]	-20	NA	NA	28	14
Supplier	PanReac	Linde Gas España SAU	-	Acros Organics	J.T. Baker
Hazards			-		

The gas used to pressurize the system was nitrogen (99.9995 % purity) and the chromatographic carrier gas was helium (99.9998 % purity), both supplied by Linde Gas España S.A.U.

4.2. CATALYST PREPARATION PROTOCOL AND CHARACTERIZATION

Following a similar procedure than the one described by Moreno Marrodan and coworkers, the catalysts were prepared by direct ion-exchange in aqueous solution [45].

Firstly, the desired amount of the dry ion exchange resin, namely A15 or Dow2, was weighted and added to a 500 mL flask containing a stirring bar. Then, the amount of precursor salt that guaranteed a certain nominal content of the metal in the catalyst, typically 1 wt.%, was added to the flask along with 400 mL of water. The resulting mixture was stirred for 4 days at room temperature. After this period, the suspension was filtrated, and the doped ion exchange resin was consecutively washed with 150 mL of deionized water, 150 mL of methanol, and 150 mL of diethyl ether. Finally, the catalyst was dried, first in an atmospheric oven at 110 °C for 3-4 h, and, afterwards, in a vacuum oven for 24 hours at 100 °C and 0.1 MPa prior to its use.

For the catalysts characterization, the following techniques and instruments have been employed:

- Inductively coupled plasma mass spectrometry (ICP-MS): It was used to determine the metal content in the ion exchange resin. The analysis was performed by Scientific and Technological Centers (CCiTUB), an independent organization in the Universitat de Barcelona group. The analysis required a dried sample of the catalyst and it was performed in an Optima 3200 rl, Perkin Elmer.
- Brunauer-Emmet-Teller (BET) analysis: Between 1 and 2 g of the dried ion exchange resins were brought to CCiTUB to determine the specific surface of the catalysts. This analysis was performed in a Micromeritics TriStar 3000 V6.04.
- Determination of the acid capacity: The acid capacity of the different ion exchange resins was determined in the lab by titration against a standard base, following a similar procedure to the one reported by Fisher and Kunin [46]. Further details regarding this procedure can be found in Annex 1.
- Transmission electron microscopy (TEM): It was used to observe the metal particles that were supported on the ion exchange surface. From the images taken, a particle size distribution was calculated. The sample that was required for the analysis was prepared in the laboratory. In this case the transmission electron microscope used was a Jeol JEM-2100 located in CCiTUB.

- Scanning electron microscopy (SEM): With this technique, the catalyst surface could be observed. Additionally, a metal mapping could be generated to see the location of the metal throughout the catalyst. A mixture of crashed and uncrashed catalysts beads were analyzed in a Jeol 6510 equipped with an EDX detector from Oxford Instruments.

4.3. SETUP

The experimental setup consisted of a 100 mL (with a 70 mL working volume) stainless-steel batch reactor (316sS Autoclave Engineers, Inc.) with a maximum operating pressure of 150 bar and 232 °C as the maximum operating temperature. A schematic diagram of the experimental installation is shown in Figure 2.

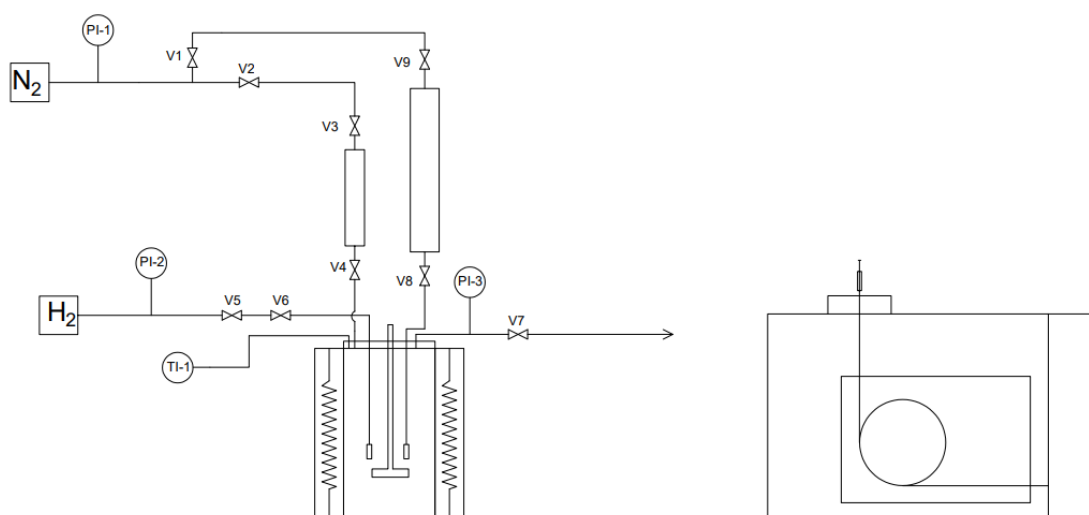


Figure 2. Schematic diagram of the batch reactor setup

The reactor was equipped with a stirrer, a pressure gauge, a rupture disk and an electric jacket, that heated the reactor. Different internals, that acted as baffles as well, could also be found in the reactor which corresponded to the hydrogen entry, the thermocouple and the sampling pipe with the respective filter.

The stirring speed and the temperature were both automatically controlled by the IB-40 Reactor Controller (Iberfluid instruments), while the pressure was manually controlled through valve 7 (V7) depending on what the pressure gauge (PI-3) indicated.

A gas chromatograph (Agilent 7890A GC System), connected to a computer, was used to analyze the product mixture. A 0.1 μL sample was manually injected in the gas

chromatograph which was equipped with a capillary column (HP-PONA, US Patent No. 4293415, USA, 50 m x 0.2 mm x 0.5 μm) and used a helium flow of 1.05 mL/min. The total run time of the analysis was of 10 minutes under isothermal conditions, at 115 °C.

4.4. CATALYTIC ACTIVITY TEST PROCEDURE

The procedure of the catalytic activity test, to produce MIBK from acetone, is shown below:

- 1) 2 g of the catalyst were loaded into the reactor vessel.
- 2) Later, 40 g of acetone were introduced to the reactor and the reactor was closed.
- 3) At this point, a leak test had to be carried out. To do so, the reactor was pressurized up to 20 barg with nitrogen through valves V2, V3 and V4. Once the nitrogen entry was closed and the pressure remained steady, the next step could be carried out.
- 4) The stirrer was turned on at 300 rpm and the reactor jacket was set at the desired temperature.
- 5) The nitrogen was removed from the reactor by carrying out 3 flushing cycles with hydrogen. Every flushing cycle consisted of depressurizing the reactor by opening V7 and, once the reactor was depressurized, hydrogen was inserted by opening V5 and V6 until the desired pressure was reached.
- 6) The hydrogen pressure was set at this point. The hydrogen pressure was set and maintained at 30 barg by leaving V6 opened, which corresponded to the hydrogen entry.
- 7) After waiting the corresponding reaction time, the electric jacket was turned off.
- 8) The hydrogen was removed by carrying out 3 flushing cycles with nitrogen.
- 9) The reactor was depressurized as soon as the temperature was below 50 °C.
- 10) Later, the stirrer was turned off.
- 11) At this point the reactor could be opened.
- 12) The reaction mixture was then filtered. Samples of 0.1 μL of the filtrate were analyzed via gas-chromatography to identify and quantify reactants and unreacted products from the reactor liquid media. The filtration cake, that

corresponded to the used catalyst, was dried after the activity test for further catalyst characterization.

4.5. REACTION CONDITIONS

Experiments lasted 4 hours, which was considered enough time to observe differences in the performance of the tested catalysts, including the commercial ACH28 and the catalysts prepared using A15 or Dow2 as supports. All experimental runs were carried out isothermally, at 120 °C, and at a constant hydrogen pressure of 30 barg, with a stirring speed of 300 rpm. The initial load consisted of 2 g of the tested catalyst and 40 g of acetone. These reaction conditions were selected based on the work presented by Talwalkar and his coworkers [18].

5. RESULTS AND DISCUSSION

In this section, the results of the catalytic activity test will be presented and discussed. Furthermore, the catalyst characterization results will be exposed to establish a more in-depth discussion of the catalytic results.

5.1. CALIBRATION

A calibration of the gas chromatograph (GC) was required to identify and quantify each substance involved in the MIBK synthesis reaction. To calibrate the system, different vials with a known mass of the different species were analyzed with a GC. With the retention time, the different species were identified while the area beneath each peak was used to establish a relationship with the mass fraction of the component.

Only the compounds observed in the different experimental runs have been calibrated in this project. Thus, since DAA was not observed in the different experimental runs it was not calibrated. The calibration equations for the different species can be found in Table 5. See Appendix 1 for their graphical representation.

Table 5. Calibration equation for the reaction species

Compound	Retention time [min]	Calibration equation ^a	R ²
Water	3.2	$A_{H_2O} = 1.1419 \cdot w_{H_2O} + 0.9664$	0.9911
Acetone	3.4	$A_{Acetone} = 0.9852 \cdot w_{Acetone} + 0.9575$	0.9952
MIBK	4.5	$A_{MIBK} = 0.9546 \cdot w_{MIBK} - 0.2082$	0.9987
MO	5.0	$A_{MO} = 0.9341 \cdot w_{MO} - 0.0581$	0.9996

^a Where w_j is the mass fraction of the compound j and A_j is the area under each peak, both expressed as a percentage

5.2. CATALYTIC ACTIVITY TEST

As mentioned above, the hydrogenation of the acetone to produce MIBK was selected as the model reaction for testing the metal-doped ion exchange resins. Results of the catalytic activity tests are shown in Figure 3.

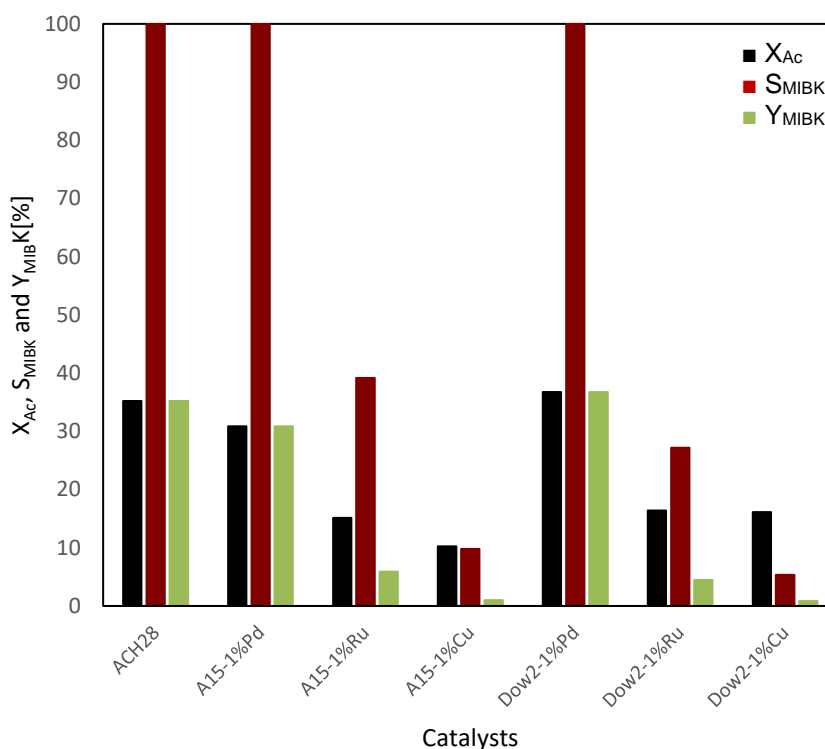


Figure 3. Catalytic activity tests ($m_{\text{acetone}} = 40$ g, catalyst load = 5 wt./wt. of acetone, $T = 120$ °C, $P_{\text{H}_2} = 30$ barg, $\omega = 300$ rpm, $t = 4$ h)

As seen in Figure 3, acetone conversion values ranged between 15 and 37 % at the end of the experimental runs, which is similar to the literature references reporting conversions of 45 % or less [18]. In fact, two different major groups of catalysts can be distinguished: on one side, Pd-doped catalysts, could convert more than 30 % of the acetone, while on the other side conversion with Cu- and Ru-doped catalysts dropped to less than 20 %. While comparing the different supports, it seems that the catalysts using Dow2 as the support tend to reach higher conversions.

With respect to selectivity, the metal supported on the ion exchange resin had a great influence in the obtained product. On one hand, resins doped with non-noble metal (that is, Cu) were less selective towards the MIBK compared to the noble metals (Pd and Ru), which can be explained on the basis of the fact that non-noble metal-based hydrogenations usually require severe reaction conditions, in terms of temperature and

hydrogen pressure [47,48]. On the other hand, concerning resins containing noble metals, palladium reached an outstanding 100 % selectivity regardless of the support, while ruthenium was far from this value. This difference has been already observed in the literature and is related to the catalytic activity in the hydrogenation of carbon double bonds, as is the case of the MO hydrogenation to obtain MIBK. In this sense, while palladium is mostly used in the hydrogenation of carbon double bonds, ruthenium is used to hydrogenate carbonyl groups [48–50]. Therefore, based on the literature and results presented herein, ruthenium catalysts should not be employed for the MIBK synthesis under the present one-pot synthesis approach.

Obviously, palladium-containing materials showed a much better yield, around 30-35 %, than ruthenium and copper catalysts, as it follows from the definition of yield.

To evaluate the catalytic activity, the TON has been calculated for all the tested catalysts (Table 6). As it can be observed, among the catalysts tested, ACH28 resulted to be the most active catalyst, followed by the Dow2-1%Pd. This difference can be explained by the catalyst load, since the metal content of ACH28 was lower than the prepared ones. Therefore, for similar acetone conversions, a higher catalytic activity was expected.

Table 6. TON of the bifunctional polymeric catalysts

Fresh catalysts	ACH28	A15-1%Pd	A15-1%Ru	A15-1%Cu	Dow2-1%Pd	Dow2-1%Ru	Dow2-1%Cu
TON [-]	1839 ^a	1190 ^b	527 ^c	244 ^b	1500 ^b	571 ^c	385 ^b

^a Using the metal content provided by the supplier [39]

^b Using the real metal content, determined by ICP-MS

^c Using the nominal content

According to Table 6, the metals supported on Dow2 tend to be more catalytically active than those supported on A15. A suitable explanation to this difference, could be the ability to swell of the gel-type resins due to the contact with polar solvents, such as acetone [51]. However, these differences can be due to the metal content, the metal size distribution or the possible loss of acidic active sites. Due to this uncertainty, a catalyst characterization was required for the prepared catalysts, as well as the commercial one.

5.3. CATALYST CHARACTERIZATION

Since both literature and activity tests showed that neither Cu- or Ru-based catalysts were inadequate for the MIBK synthesis, the focus in characterization was set on Pd catalysts. Cu-based catalysts were also characterized for the sake of comparison.

Among the prepared catalysts, both fresh and used catalysts were characterized. The commercial catalyst, ACH28, was only characterized after its use because some data on its morphological features were either available from previous works or provided by the supplier.

In Table 7, the results of the ICP-MS and BET analysis are presented along the acid capacity of each catalyst. The specific surface of the copper-containing resins is still pending to be characterized.

Table 7. Catalyst characterization

Characterized catalysts	ICP-MS ^a		BET ^c		Acid capacity ^d	
	[metal wt.%]		[m ² /g]		[meqH ⁺ /g]	
	Fresh	Used	Fresh	Used	Fresh	Used
ACH28	0.70 ^b	0.61	36 ^b	1.2742	4.80 ^b	-
A15	-	-	46.558	-	4.81 ^e	-
A15-1%Pd	0.95	0.95	50.280	45.899	4.63±0.14	4.57±0.13
A15-1%Cu	0.9	0.08	-	-	4.77±0.03	4.801±0.012
Dow2	-	-	1.553	-	4.98 ^e	-
Dow2-1%Pd	0.89	0.87	0.1103	0.1304	4.77±0.09	4.78±0.09
Dow2-1%Cu	0.92	0.21	-	-	4.98±0.07	4.999±0.064

^a Unless otherwise indicated, data obtained by the metal analysis unit, in CCiTUB .

^b Data obtained from the supplier [39].

^c Unless otherwise indicated, data obtained by the unit of polymorphism and calorimetry, in CCiTUB.

^d Unless otherwise indicated, data obtained experimentally in the laboratory.

^e Data obtained from the literature [51].

The metal content on the fresh catalysts indicates that 89-95 % of the metal was successfully anchored to the catalyst polymer matrix and, consequently, both nominal and actual metal content were about 1 wt.%. Focusing on ICP-MS results on used catalysts, it can be observed that palladium-containing resins suffered no significant

metal loss during the catalytic activity test while the copper contained in the copper-based resins decreased significantly, which reveals that leaching phenomenon took place in those catalysts.

In the present work, BET analysis showed significant differences between prepared catalysts and the commercial ACH28. For instance, the specific area of fresh A15-1%Pd samples is $50.28 \text{ m}^2/\text{g}$, which is consistent with A15 specific area before introduction of the metal (that is, according to the supplier, $53 \text{ m}^2/\text{g}$) but, on the other hand, ACH28 specific area is $36 \text{ m}^2/\text{g}$. Furthermore, after the catalytic test, the specific area of A15-1%Pd slightly drops to $45.9 \text{ m}^2/\text{g}$, whereas ACH28 sinks to only $1.274 \text{ m}^2/\text{g}$ [37,39]. Regarding gel-type resins, Dow2 specific surface was $1.553 \text{ m}^2/\text{g}$ before introduction of the metal, and that it maintained at about $0.1 \text{ m}^2/\text{g}$ after palladium was anchored. These values are completely consistent with the nature of this polymeric matrix, typically collapsed in dry condition. The obtained specific surface value for ACH28 after the catalytic activity test is somewhat surprising and needs further reevaluation (which is currently in progress) but, so far, results would indicate that either the catalyst pores were blocked during reaction (perhaps due to accumulation of heavy compounds), or that some structural damage was caused on the resin matrix. The former explanation seems inadequate due to the fact that no heavy compounds were ever detected in any GC analysis, while the latter has not been reported in previous literature references.

When comparing the acid capacity of the different catalysts, it can be observed how the acid capacity did not change during the catalytic activity test. In this case, though, a difference in the acid capacity between the catalysts is observed, since the catalysts doped with palladium are less acid than those doped with copper. The ion exchange resins have an acid capacity of $4.81 \text{ meqH}^+/\text{g}$ for A15 whereas the value for the Dow2 was of $4.98 \text{ meqH}^+/\text{g}$ according to the suppliers [37,51]. Therefore, the results suggest that the palladium precursor salt decreased the acidic sites of the polymeric support due to the ion exchange that took place in the catalyst preparation.

The metal nanoclusters average sizes were determined from the TEM images. Several TEM images of the prepared can be found in Appendix 4. In Table 8, the average metal size of the different catalysts is shown.

Table 8. Average metal size.

Catalysts	Particle size ^a [nm]	
	Fresh	Used
ACH28	6.2±0.2	12.5 ± 0.4
A15-1%Pd	20.2 ± 0.6	4.54 ± 0.07
A15-1%Cu	7.3 ± 0.3	9.9 ± 0.3
Dow2-1%Pd	8.5 ± 0.2	6.15 ± 0.13
Dow2-1%Cu	N/C	N/C

^a Results have been obtained from more than 200 metal particles in TEM images
N/C stands for not calculated.

Firstly, it must be said that the results obtained for the palladium average size on A15 prior to the catalytic test do not seem reliable and are, therefore, currently under further revision. In this regard, obtained results indicate that the metal particles have an average particle diameter of 20 nm, which is far superior than the rest. These results are not consistent because the greater the particle is, the less available surface exists, thus worse catalytic performance is expected, which does not hold. In addition, the same analysis on the used catalyst sample produced an average particle size of 4 nm, much smaller than original particles in the fresh sample. Notice that previous literature reports on metal nanoclusters forming larger aggregates upon reaction, not smaller.

When comparing the impact that the catalytic activity test had on the average metal size, it has been observed that the metal size for ACH28 and A15-1%Cu increased, possibly due to the aggregation of the smallest nanoparticles. On the other hand, for the A15-1%Pd and Dow2-1%Pd the obtained average size of the metal particles decreased. Regarding A15-1%Pd, it has already been mentioned that results are being further studied at present. With respect to Dow2-1%Pd, the change in metal average size can be is small enough to consider it as not significant, since the detected differences could be related to sampling.

Regarding Dow2-1%Cu average size distribution, which is missing in Table 8, it should be indicated that metal average size distribution could not be calculated for several reasons. In the first place, metal aggregates were observed which hindered the particle measurement. Also, the electron beam used for the TEM measurements melted the ion

exchange resin support. Furthermore, the crystalline planes were observed difficulting the particle measurement. Prove of these problems can be observed in Figure 4.

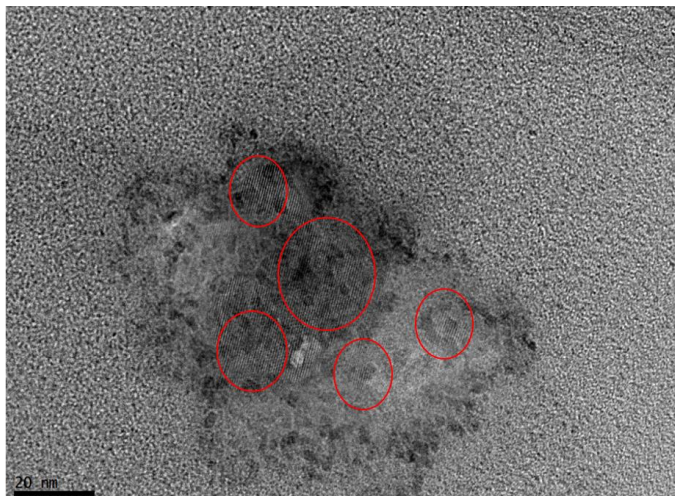


Figure 4. TEM image of copper supported on Dow2

As it can be appreciated in Figure 4, the copper was found in metal aggregates. In the present picture, it can be observed different black dots that correspond to copper particles. Alternatively, the red circles show different parallel lines that correspond to the crystalline planes of the metal, making it difficult to distinguish the metal particles and the amorphous support.

TEM images and the corresponding metal size distribution of A15-1%Pd and Dow2-1%Pd, the two best-performing prepared catalysts, are shown in Figures 5 and 6, respectively, before and after the catalytic test. The prepared catalysts metal size distribution can be found in Appendix 5.

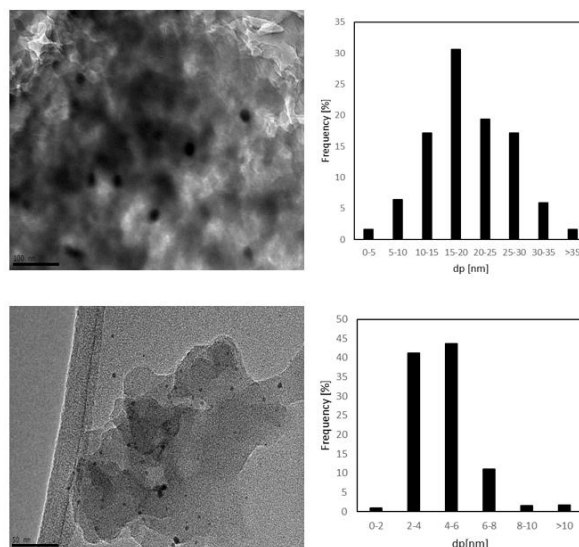


Figure 5. TEM image and palladium size distribution of A15-1%Pd, before the catalytic activity test (top images) and after the catalytic activity test (bottom images)

From Figure 5, it can be observed how the palladium metal particles were much bigger before the catalytic activity test than after. Focusing on the particle size distribution before the catalytic activity test, it can be observed how most of the particles have a diameter between 15 and 20 nm, which is much bigger than what was anticipated. Therefore, as commented in previous lines, these results are currently being under reevaluation. Surprisingly, metal average size for the used catalyst sample was far smaller, which is consistent with the relatively good catalytic results obtained. As indicated before, this variation in average size is yet to be confirmed since it could be caused by deficient sampling but, if confirmed, it could entail redistribution of the metal nanoparticles under reaction conditions.

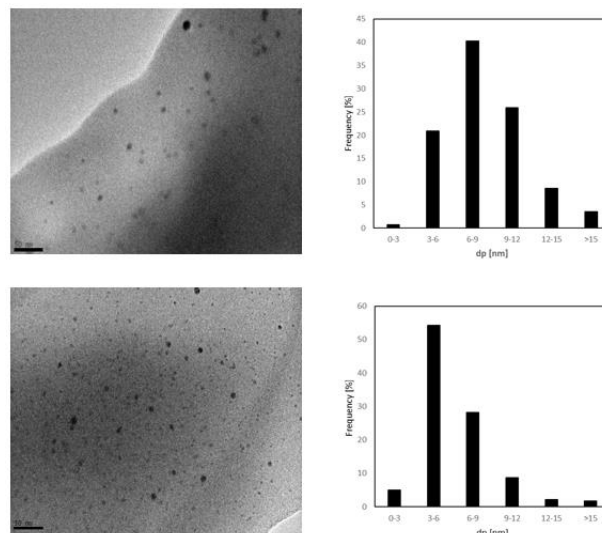


Figure 6. TEM image and palladium size distribution of Dow2-1%Pd, before the catalytic activity test (top images) and after the catalytic activity test (bottom images)

Regarding Dow2-1%Pd in Figure 6, it is worth noting that although the catalyst was prepared by direct ion-exchange in aqueous medium, which is one of the simplest reported techniques, it can be observed how the palladium metal particles were homogeneously dispersed throughout the catalyst surface, as it has already been described in the literature for metal-doped gel-type resins [52–54]. From the TEM images, no metal aggregates can be seen, which involves that more available metallic surface was exposed. In addition, smaller particle sizes are present after the catalytic test, as evidenced by the sizes distribution histogram, with the gaussian curve shifted towards smaller sizes. As a matter of fact, more than half of the observed particles had a particle diameter between 3 and 6 nm.

Regarding the metal average size of ACH28 (Figure 7), an increase in size is observed after the catalytic test. For instance, before the catalytic test, no palladium particles were observed above 14 nm, while after the catalytic activity test, 36 % of the particles were larger than this value, which involves metal aggregation during reaction conditions. Regarding metal dispersion, metal particles were quite homogeneously distributed throughout the polymer matrix before and after the catalytic test.

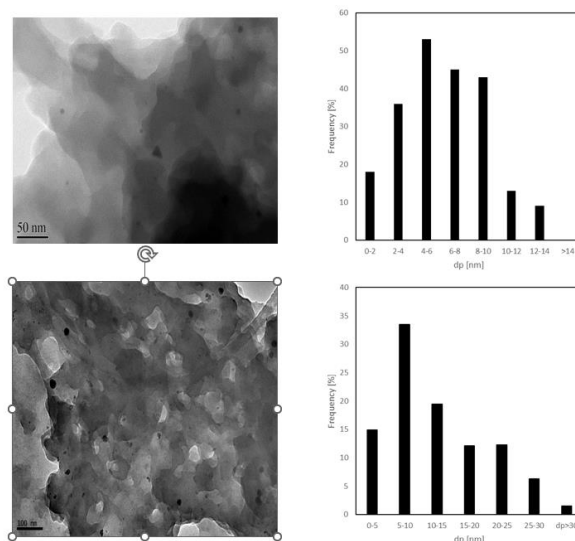


Figure 7. TEM image and palladium size distribution of ACH28 before (top) and after (bottom) the catalytic activity test

In conclusion, the outstanding performance of the Dow2-1%Pd catalyst compared to the rest of catalyst samples prepared in the present work can be attributed to both a more homogeneous distribution of the metal in the polymer matrix and to a smaller average metal nanoparticle size. Compared to ACH28, the slightly better behavior of Dow2-1%Pd can be attributed to its slightly superior amount of palladium, together with said more homogeneous distribution.

In order to further understand the better behavior of Dow2-1%Pd catalyst compared to the rest of prepared catalysts, SEM microscope technique was applied to elucidate if there were differences regarding the location of the metal within the catalyst, which ideally would be in both, the inner and outer part of the catalyst shell. SEM analyses allow metal mapping on the catalyst (which can be found in Appendix 5). In Figure 8 and 9, the SEM images as well as the palladium mapping of the Dow2-1%Pd and A15-1%Pd are shown.

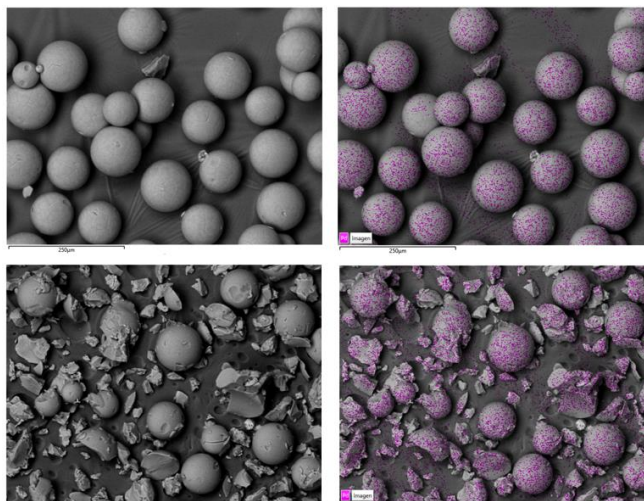


Figure 8. SEM images and Pd mapping for the Dow2-1%Pd catalyst, before (top images) and after (bottom images) the catalytic activity test.

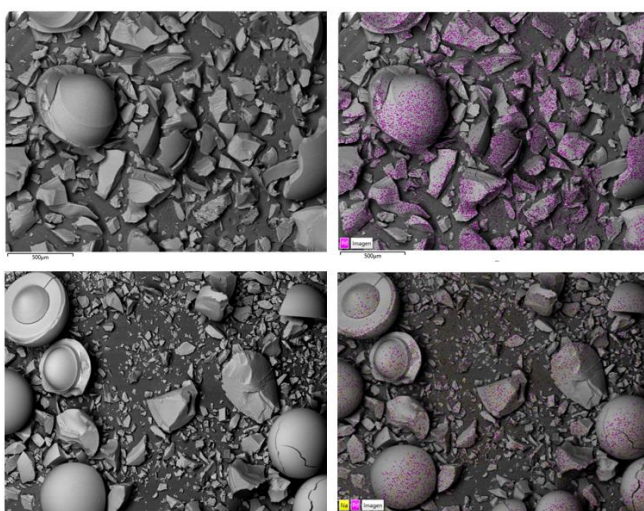


Figure 9. SEM images and Pd mapping for the A15-1%Pd catalyst, before (top images) and after (bottom images) the catalytic activity test.

In Figure 8, a mixture of crushed and uncrushed catalyst beads are shown. Although some beads were intentionally crushed, it is observed how the catalytic activity test provoked a mechanical stress on the catalyst, since more attrition is observed. Focusing now on the mapping of the metal, it can be seen how the palladium was found in the inner and outer part of the catalyst wall. Therefore, palladium was homogeneously distributed on the catalyst surface during its preparation.

As seen with the Dow2-1%Pd (Figure 8), A15-1%Pd (Figure 9) suffered mechanical stress during the catalytic activity test, although some beads were intentionally crushed. In this case, the palladium can also be found in the inner and outer part of the catalyst walls.

In terms of yield towards MIBK, Dow2-1%Pd resulted to be the most adequate catalyst among the prepared catalysts. The highest yield was achieved by this catalyst as well as it had the highest TON, 1500 moles of acetone converted per mol of metal on the support, among the prepared catalysts. Furthermore, it had the smallest average size which makes it a good catalyst for the reaction.

5.4. CATALYTIC ACTIVITY TEST AT DIFFERENT OPERATING TEMPERATURES

An important property of the heterogeneous catalysts is the versatility of the operating conditions at which the catalysts can successfully work. Since Dow2-1%Pd was identified as the best performing catalyst, in terms of conversion and yield towards the product of interest, further experiments were performed with this catalyst to evaluate its performance at different operating temperatures. The tested temperatures were 110 °C, 120 °C and 130 °C, while the other operating conditions remained constant. Results are shown in Figure 10.

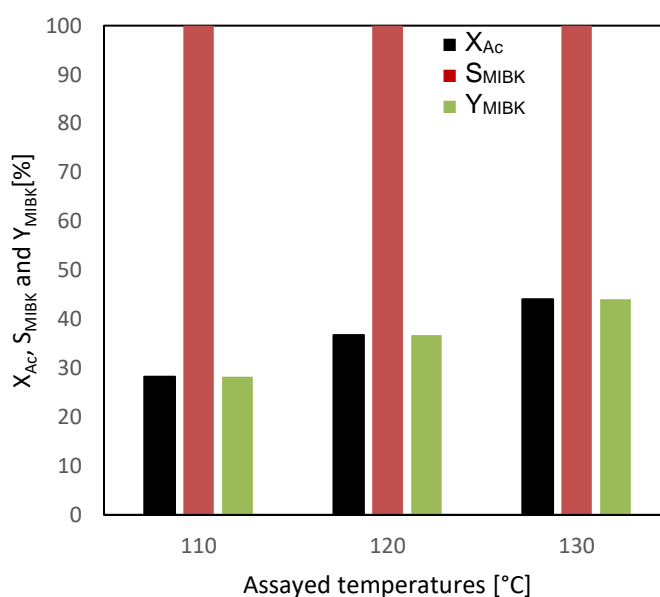


Figure 10. Dow2-1%Pd catalytic activity at different temperatures ($m_{\text{acetone}} = 40$ g, catalyst load = 5 wt./wt. of acetone, $P_{\text{H}_2} = 30$ barg, $\omega = 300$ rpm, $t = 4$ h).

As expected, acetone conversion increased with increasing temperature. Although the literature says that an increment of the conversion is at the cost of the selectivity [18], in the studied temperature range the formation of products such as MO or DAA was not observed. From that it follows that increasing temperature resulted in an increase in yield towards MIBK.

5.5. CATALYST REUSE

Since the reusability of a catalyst is an important matter from an industrial point of view, it was proposed to carry out a reusability test on the best catalyst, Dow2-1%Pd. This test consists of performing catalytic activity test runs, maintaining the same operating conditions, but for three consecutive cycles. To do so, at the end of each experimental run, the catalyst was separated and dried at room temperature for 24 hours before using it again. In Figure 11, the results of the reusability test can be found.

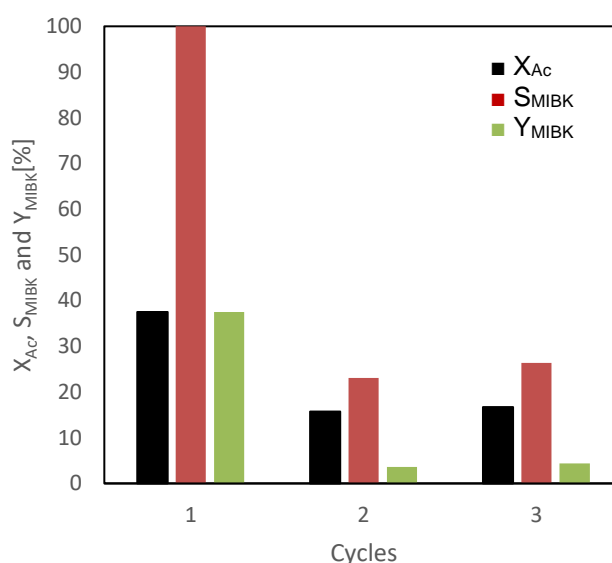


Figure 11. Results of the reusability test of the Dow2-1%Pd catalyst. ($m_{acetone} = 40$ g, catalyst load = 5 wt./wt. of acetone, $T = 120$ °C, $P_{H_2} = 30$ barg, $\omega = 300$ rpm, $t = 4$ h)

Figure 11 shows how the prepared catalyst are not suitable to be reused. When the catalyst is fresh, similar results to the catalytic activity test, in terms of acetone conversion (37 %) and selectivity (100%), and consequently yield (37 %), towards MIBK are observed. But at the second cycle acetone conversion drops drastically to about 20 %. Selectivity towards the product of interest also decayed significantly, which suggests catalyst deactivation. In the literature, it is proposed that a catalyst gets deactivated during the course of the reaction due to the presence of non-polar solvents, such as water, which adsorbs on the resin surface covering the catalytic sites, therefore, causing the inhibition effect [18].

In the aim to see the cause of the difference in the acetone conversion, the catalyst was recovered and dried. However, only half of the catalyst load in the first cycle had been recovered, showing that the separation procedure had not been efficient enough.

In the aim to compare the catalytic activity within the different reuse cycle, the results had to be normalized per gram of catalyst. In Figure 12, the normalized results can be observed.

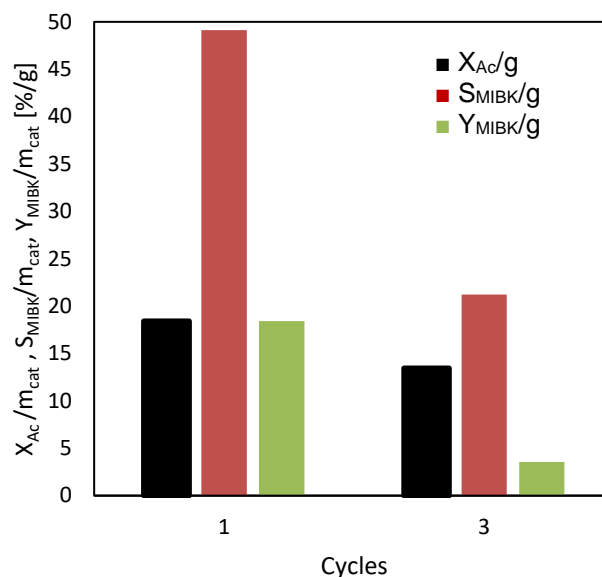


Figure 12. Normalized results of the catalytic activity test while reusing the catalyst ($m_{acetone} = 40$ g, catalyst load = 5 wt./wt. of acetone, $T = 120$ °C, $P_{H_2} = 30$ barg, $\omega = 300$ rpm, $t = 4$ h).

In Figure 12, it can be observed how the acetone conversion per gram of catalyst in the third cycle was similar to the one achieved in the first run, which means that if the catalyst had been efficiently recovered, a similar acetone conversion could have been achieved. Therefore, the main contribution to the observed lower conversion in every cycle is simply related to the catalyst mass loss, rather than to the impact of the water presence, as suggested by the literature.

On the other hand, it can be observed a significant loss of selectivity towards the product of interest. Although no other species, including MO and DAA, other than MIBK were observed in the reaction medium, its production decreased significantly within the different cycles while the mass fraction of water increased significantly. From these results, it can be assumed that some of the converted acetone did not form MIBK, but instead some dehydration step took place, which would explain the increase of the water content in the final mixture.

The TON was also calculated in this case. In the first cycle it reached a value of 1517 moles of acetone converted by a mol of metal while in the third cycle it had a value of

1211. As it can be observed a slightly loss of catalytic activity occurred between the different cycles.

In addition, the metal contained in the ion exchange resin was determined after the third cycle by ICP-MS. This analysis showed that the catalyst had a metal content of 0.81 %, which compared to the initial figure of about 0.89 % suggests almost insignificant leaching.

This test suggested a catalyst deactivation within the different experimental runs. Since the ICP-MS stated that no leaching of the metal took place during the first cycle, the cause of the deactivation of the catalyst should not be the metal loss. To see the location of the metal, the catalyst after the third cycle was analyzed by SEM. In Figure 13, an image of the catalyst and mapping of the metal can be observed.

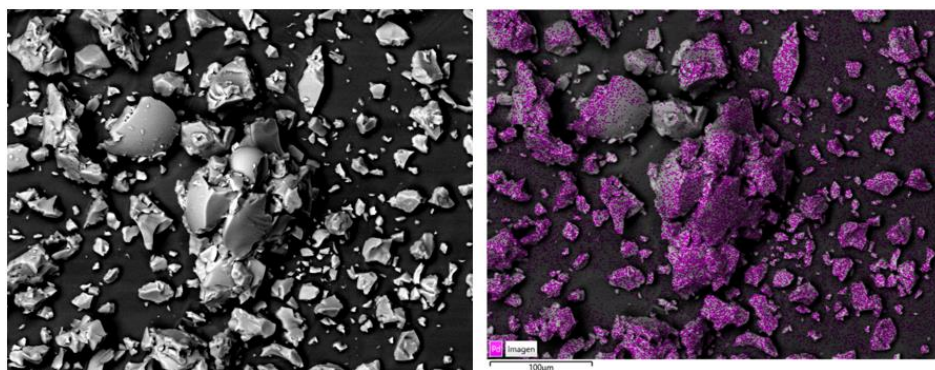


Figure 13. Catalyst SEM image (left) and palladium mapping (right).

Although some beads were crashed intentionally, more attrition can be observed at the end of the third cycle, which is logical since the catalyst underwent more mechanical stress. Focusing on the palladium mapping, it can be concluded that the palladium was present in throughout the catalyst since its presence can be found in both, inner and outer, layers of the catalyst.

According to the obtained results, the prepared catalyst was not fit to be reused since, although it showed a similar acetone conversion level per gram of catalyst, it was unable to synthesize MIBK. Contrarily, references can be found in the literature reporting up to 6 different cycles without showing any significant catalytic activity loss with catalysts prepared through similar procedures, but in different hydrogenation model reactions [55].

In conclusion, the Dow2-1%Pd sample is not fit to be reused several times due to the decrease in the selectivity towards the product of interest. Nevertheless, it can be efficiently used in one cycle having a similar catalytic activity compared to a commercial catalyst, namely ACH28.

6. CONCLUSIONS AND FUTURE WORK

The present work was focused on the preparation of bifunction catalysts, using ion exchange resins as a support, for the transformation of biomass-derived products under the one-pot synthesis approach, where the MIBK production was selected as a model reaction.

Firstly, three different metals (Pd, Ru and Cu) were successfully doped in the commercial supports, namely A15 and Dow2, with a nominal content of 1 wt.%. It was proven that all the catalysts possessed catalytic activity, where the non-noble metals were the least active since severe conditions are needed. Among the noble metals, the palladium doped resins were the most active catalysts since palladium is used for hydrogenating C=C bonds while ruthenium is used for the hydrogenation of carbonyl groups. Of the different prepared catalysts, Dow2-1%Pd achieved the highest acetone conversion (37%) while being the most selective towards MIBK (100%). In fact, it was the most catalytically active according the TON number, which reached a value of 1500.

Secondly, the prepared catalysts were compared to a commercial bifunctional catalysts, namely ACH28. Although the commercial catalysts achieved similar conversions and selectivity towards the product of interest as the prepared catalysts, it was more active in catalytical terms since the TON had a value of 1839. The TON was higher because its metal content of the commercial catalyst was lower than the prepared catalysts.

Thirdly, these catalysts were characterized by different techniques. The ICP-MS analysis showed that the metal was successfully doped in the catalyst with a metal mass content around 0.9 %, close to the nominal content of 1 wt.%. Additionally, it also showed that no leaching took place with the palladium doped resins while for the copper doped catalysts, the metal loss was significant. It was also observed how no loss of acidic sites took place during the reaction, but a lower acidity compared to the metal-free supports was observed for the catalysts doped with palladium. The specific surface of the metal was also observed but the results were not consistent since the ion exchange resin was not swollen, therefore, the specific surfaces were lower than the surface provided by the supplier.

Then, the catalyst underwent SEM and TEM images. These techniques proved that the different metals were present throughout the ion exchange resins in both, the inner and outer, part of the shell. The TEM images showed how the metal was homogeneously dispersed throughout the supports and from its images the metal size distribution was done. It was seen how the metal particles in the Dow2 support are small (8.495 ± 0.220 nm), therefore, it has more metallic surface which eventually makes Dow2-1%Pd a good catalyst.

Lastly, the Dow2-1%Pd, the best prepared catalyst, underwent a catalytic activity test at different operating temperatures and the potential reuse of it was tested. The first test proved how the acetone conversion was increased with an increase in temperature without a selective loss in the studied temperature range. The catalyst reuse showed a loss of selectivity towards MIBK, although it achieved similar acetone conversions which means that it conserved its catalytic activity. Therefore, the reuse of the prepared catalyst is not feasible.

As for the future work, at short term to continue with the study, the prepared catalyst would be analyzed by x-ray diffraction to observe the crystal morphology. In addition, there are some samples that require a repetition of the TEM analysis. The BET analysis of the palladium containing resins need to be repeated while for the copper containing resins need to be done.

At a long-term period, the tested catalyst would need to be assayed in a continuous reactor. Then, the catalysts should be prepared with a lower metal content to reduce its cost. In addition, the hydrogen pressure should be lowered to increase the safety of the reaction.

7. REFERENCES

1. Pfaltzgraff, L.A.; Clark, J.H. *Green Chemistry, Biorefineries and Second Generation Strategies for Re-Use of Waste: An Overview*; **2014**; ISBN 9780857095213.
2. Jing, Y.; Guo, Y.; Xia, Q.; Liu, X.; Wang, Y. Catalytic Production of Value-Added Chemicals and Liquid Fuels from Lignocellulosic Biomass. *Chem* **2019**, *5*, 2520–2546, doi:10.1016/j.chempr.2019.05.022.
3. Yen, H.W.; Li, R.J.; Ma, T.W. The Development Process for a Continuous Acetone-Butanol-Ethanol (ABE) Fermentation by Immobilized *Clostridium Acetobutylicum*. *J. Taiwan Inst. Chem. Eng.* **2011**, *42*, 902–907, doi:10.1016/j.jtice.2011.05.006.
4. Hommes, A.; Heeres, H.J.; Yue, J. Catalytic Transformation of Biomass Derivatives to Value-Added Chemicals and Fuels in Continuous Flow Microreactors. *ChemCatChem* **2019**, *11*, 4671–4708, doi:10.1002/cctc.201900807.
5. Sarangi, P.K.; Nanda, S.; Mohanty, P. *Recent Advancements in Biofuels and Bioenergy Utilization*; **2018**; ISBN 9789811313073.
6. Démolis, A. Synthèse Catalytique de Lévinates de Butyle à Partir de Biomasse En Présence d'alcools Ou d'oléfines. *Univ. Lyon* **2017**.
7. Climent, M.J.; Corma, A.; Iborra, S. Conversion of Biomass Platform Molecules into Fuel Additives and Liquid Hydrocarbon Fuels. *Green Chem.* **2014**, *16*, 516–547, doi:10.1039/c3gc41492b.
8. Corma Canos, A.; Iborra, S.; Velty, A. Chemical Routes for the Transformation of Biomass into Chemicals. *Chem. Rev.* **2007**, *107*, 2411–2502, doi:10.1021/cr050989d.
9. Mahapatra, M.K.; Kumar, A. A Short Review on Biobutanol, a Second Generation Biofuel Production from Lignocellulosic Biomass. *J. Clean Energy Technol.* **2017**, *5*, 27–30, doi:10.18178/jocet.2017.5.1.338.
10. Doran-Peterson, J.; Cook, D.M.; Brandon, S.K. Microbial Conversion of Sugars from Plant Biomass to Lactic Acid or Ethanol. *Plant J.* **2008**, *54*, 582–592, doi:10.1111/j.1365-313X.2008.03480.x.
11. Cardona Alzate, C.A.; Solarte Toro, J.C.; Peña, Á.G. Fermentation,

- Thermochemical and Catalytic Processes in the Transformation of Biomass through Efficient Biorefineries. *Catal. Today* **2018**, *302*, 61–72, doi:10.1016/j.cattod.2017.09.034.
12. Johanson, G. *Patty's Toxicology*; 2012; Vol. 3;.
 13. Liew, F.E.; Nogle, R.; Abdalla, T.; Rasor, B.J.; Canter, C.; Jensen, R.O.; Wang, L.; Strutz, J.; Chirania, P.; De Tissera, S.; et al. Carbon-Negative Production of Acetone and Isopropanol by Gas Fermentation at Industrial Pilot Scale. *Nat. Biotechnol.* **2022**, *40*, 335–344, doi:10.1038/s41587-021-01195-w.
 14. Howard, W.L. Acetone. *Kirk-Othmer Encycl. Chem. Technol.* **2011**, 1–15.
 15. Veza, I.; Muhamad Said, M.F.; Latiff, Z.A. Recent Advances in Butanol Production by Acetone-Butanol-Ethanol (ABE) Fermentation. *Biomass and Bioenergy* **2021**, *144*, doi:https://doi.org/10.1016/j.biombioe.2020.105919.
 16. Werpy, T.; Petersen, G. Top Value Added Chemicals from Biomass. *U.S Dep. Energy Energy Effic. Renew. Energy* **2004**, *1*, 1–76, doi:10.2172/15008859.
 17. Liguori, F.; Oldani, C.; Capozzoli, L.; Calisi, N.; Barbaro, P. Liquid-Phase Synthesis of Methyl Isobutyl Ketone over Bifunctional Heterogeneous Catalysts Comprising Cross-Linked Perfluorinated Sulfonic Acid Aquivon Polymers and Supported Pd Nanoparticles. *Appl. Catal. A Gen.* **2021**, *610*, 117957.
 18. Talwalkar, S.; Mahajani, S. Synthesis of Methyl Isobutyl Ketone from Acetone over Metal-Doped Ion Exchange Resin Catalyst. *Appl. Catal. A Gen.* **2006**, *302*, 140–148.
 19. Wang, P.; Bai, S.; Zhao, J.; Su, P.; Yang, Q.; Li, C. Bifunctionalized Hollow Nanospheres for the One-Pot Synthesis of Methyl Isobutyl Ketone from Acetone. *ChemSusChem* **2012**, *5*, 2390–2396, doi:10.1002/cssc.201200383.
 20. Trejo, J.A.; Tate, J.; Martenak, D.; Huby, F.; Baxter, S.M.; Schultz, A.K.; Olsen, R.J. State of the Art Bifunctional Hydrogenation Heterogeneous Polymeric Catalyst. *Top. Catal.* **2010**, *53*, 1156–1162, doi:10.1007/s11244-010-9553-1.
 21. Izquierdo, J.F.; Cunill, F.; Tejero, J.; Iborra, M.; Fité, C. *Cinética de Las Reacciones Químicas*; 16th ed.; Edicions de la Universitat de Barcelona: Barcelona, **2004**; ISBN 978-87-8338-479-4.
 22. Climent, M.J.; Corma, A.; Iborra, S. Mono-and Multisite Solid Catalysts in

- Cascade Reactions for Chemical Process Intensification. *ChemSusChem* **2009**, *2*, 500–506, doi:10.1002/cssc.200800259.
23. Felpin, F.X.; Fouquet, E. Heterogeneous Multifunctional Catalysts for Tandem Processes: An Approach toward Sustainability. *ChemSusChem* **2008**, *1*, 718–724, doi:10.1002/cssc.200800110.
 24. Démolis, A.; Essayem, N.; Rataboul, F. Synthesis and Applications of Alkyl Levulinates. *ACS Sustain. Chem. Eng.* **2014**, *2*, 1338–1352, doi:10.1021/sc500082n.
 25. Akelah, A.; Sherrington, D.C. *Application of Functionalized Polymers in Organic Synthesis*; **1981**; Vol. 81; ISBN 8110781055.
 26. Soto, R. Simultaneous Etherification of C4 and C5 Fractions Using Bioethanol for Greener Fuels. *PhD Thesis* **2017**, 304.
 27. Badia, J.H. Synthesis of Ethers as Oxygenated Additives for the Gasoline Pool. **2016**, 252.
 28. Zagorodni, A.A. *Ion Exchange Materials Properties and Applications*; Elsevier, **2007**; Vol. 4; ISBN 978-0-08-044552-6.
 29. Corain, B.; Zecca, M.; Jeřábek, K. Catalysis and Polymer Networks - The Role of Morphology and Molecular Accessibility. *J. Mol. Catal. A Chem.* **2001**, *177*, 3–20, doi:10.1016/S1381-1169(01)00305-3.
 30. Kilislioglu, A. *Ion Exchange Technologies*; **2012**; ISBN 9789535108368.
 31. Higashio, Y.; Nakayama, T. One-Step Synthesis of Methyl Isobutyl Ketone Catalyzed by Palladium Supported on Niobic Acid. *Catal. Today* **1996**, *28*, 127–131, doi:10.1016/0920-5861(95)00219-7.
 32. Chen, Y.Z.; Liaw, B.J.; Tan, H.R.; Shen, K.L. One-Step Synthesis of Methyl Isobutyl Ketone from Acetone and Hydrogen over Pd/(Nb₂O₅/SiO₂) Catalysts. *Appl. Catal. A Gen.* **2001**, *205*, 61–69, doi:10.1016/S0926-860X(00)00545-7.
 33. Hetterley, R.D.; Kozhevnikova, E.F.; Kozhevnikov, I. V. Multifunctional Catalysis by Pd-Polyoxometalate: One-Step Conversion of Acetone to Methyl Isobutyl Ketone. *Chem. Commun.* **2006**, 782–784, doi:10.1039/b515325e.
 34. Kozhevnikova, E.F.; Kozhevnikov, I. V. One-Step Synthesis of Methyl Isobutyl Ketone from Acetone Catalysed by Pd Supported on ZnII-CrIII Mixed Oxide. *J.*

- Catal.* **2006**, *238*, 286–292, doi:10.1016/j.jcat.2005.11.028.
35. Al-Wadaani, F.; Kozhevnikova, E.F.; Kozhevnikov, I. V. Pd Supported on ZnII-CrIII Mixed Oxide as a Catalyst for One-Step Synthesis of Methyl Isobutyl Ketone. *J. Catal.* **2008**, *257*, 199–205, doi:10.1016/j.jcat.2008.04.025.
36. Bligaard, T.; Bullock, R.M.; Campbell, C.T.; Chen, J.G.; Gates, B.C.; Gorte, R.J.; Jones, C.W.; Jones, W.D.; Kitchin, J.R.; Scott, S.L. Toward Benchmarking in Catalysis Science: Best Practices, Challenges, and Opportunities. *ACS Catal.* **2016**, *6*, 2590–2602, doi:10.1021/acscatal.6b00183.
37. DuPont AMBERLYST™ 15 **2022**, 1–2.
38. Dow Chemical Water Solutions DOWEX™ Fine Mesh Spherical Ion Exchange Resins For Fine Chemical and Pharmaceutical Column Separations. *Dow Water Solut.* 1–9.
39. DuPont Amberlyst™ CH28 **2022**, 2–4.
40. AppliChem, P. Acetone Technical Grade Transport Data Sheet 2011.
41. Linde Hydrogen Safety Data Sheet **2022**, 1–10.
42. LabChem Water Safety Data Sheet **2020**.
43. Thermo Fisher Scientific Mesityl Oxide Safety Data Sheet **2021**.
44. Thermo Fisher Scientific Methyl Isobutyl Ketone Safety Data Sheet. **2021**.
45. Moreno-Marrodan, C.; Barbaro, P. Energy Efficient Continuous Production of γ -Valerolactone by Bifunctional Metal/Acid Catalysis in One Pot. *Green Chem.* **2014**, *16*, 3434–3438, doi:10.1039/c4gc00298a.
46. Fisher, S.; Kunin, R. Routine Exchange Capacity Determinations of Ion Exchange Resins. *Anal. Chem.* **1955**, *27*, 1191–1194, doi:10.1021/ac60103a052.
47. Simanullang, W.F.; Itahara, H.; Takahashi, N.; Kosaka, S.; Shimizu, K.I.; Furukawa, S. Highly Active and Noble-Metal-Alternative Hydrogenation Catalysts Prepared by Dealloying Ni-Si Intermetallic Compounds. *Chem. Commun.* **2019**, *55*, 13999–14002, doi:10.1039/c9cc07862b.
48. Weissemel, K.; Arpe, H.J. *Industrial Organic Chemistry*; VCH, Ed.; 3rd Editio.; Weinheim, **1997**; ISBN 9781119130536.
49. Seki, T.; Grunwaldt, J.D.; Van Vegten, N.; Baiker, A. Palladium Supported on an Acidic Resin: A Unique Bifunctional Catalyst for the Continuous Catalytic

- Hydrogenation of Organic Compounds in Supercritical Carbon Dioxide. *Adv. Synth. Catal.* **2008**, *350*, 691–705, doi:10.1002/adsc.200700532.
50. Hetterley, R.D.; Mackey, R.; Jones, J.T.A.; Khimyak, Y.Z.; Fogg, A.M.; Kozhevnikov, I. V. One-Step Conversion of Acetone to Methyl Isobutyl Ketone over Pd-Mixed Oxide Catalysts Prepared from Novel Layered Double Hydroxides. *J. Catal.* **2008**, *258*, 250–255, doi:10.1016/j.jcat.2008.06.017.
51. Ramírez, E.; Soto, R.; Bringué, R.; Iborra, M.; Tejero, J. Catalytic Hydroxyalkylation/Alkylation of 2-Methylfuran with Butanal to Form a Biodiesel Precursor Using Acidic Ion-Exchange Resins. *Ind. Eng. Chem. Res.* **2020**, *59*, 20676–20685, doi:10.1021/acs.iecr.0c04308.
52. Corain, B.; Zecca, M.; Canton, P.; Centomo, P. Synthesis and Catalytic Activity of Metal Nanoclusters inside Functional Resins: An Endeavour Lasting 15 Years. *Philos. Trans. R. Soc. A Math. Phys. Eng. Sci.* **2010**, *368*, 1495–1507, doi:10.1098/rsta.2009.0278.
53. Biffis, B.A.; Archivio, A.A.D.; Jerábek, K.; Schmid, G.; Corain, B. The Generation of Size-Controlled Palladium Nanoclusters Inside Gel-Type Functional Resins: Arguments and Preliminary Results. *Adv. Mater.* **2000**, 1909–1912.
54. Biffis, A.; Landes, H.; Jeřábek, K.; Corain, B. Metal Palladium Dispersed inside Macroporous Ion-Exchange Resins: The Issue of the Accessibility to Gaseous Reactants. *J. Mol. Catal. A Chem.* **2000**, *151*, 283–288, doi:10.1016/S1381-1169(99)00268-X.
55. Marrodan, C.M.; Berti, D.; Liguori, F.; Barbaro, P. In Situ Generation of Resin-Supported Pd Nanoparticles under Mild Catalytic Conditions: A Green Route to Highly Efficient, Reusable Hydrogenation Catalysts. *Catal. Sci. Technol.* **2012**, *2*, 2279–2290, doi:10.1039/c2cy20205k.

ACRONYMS

A15	Amberlyst™ 15
A15-1%Cu	Amberlyst™ 15 doped with copper (1 wt.%)
A15-1%Pd	Amberlyst™ 15 doped with palladium (1 wt.%)
A15-1%Ru	Amberlyst™ 15 doped with ruthenium (1 wt.%)
ACH28	Amberlyst™ CH28
BET	Brunauer-Emmet-Teller Analysis
DAA	Diacetone alcohol
Dow2	Dowex 50WX2
Dow2-1%Cu	Dowex 50WX2 doped with copper (1 wt.%)
Dow2-1%Pd	Dowex 50WX2 doped with palladium (1 wt.%)
Dow2-1%Ru	Dowex 50WX2 doped with ruthenium (1 wt.%)
ICP-MS	Inductively coupled plasma mass spectrometry
KHP	Potassium hydrogen phthalate
MIBK	Methyl isobutyl ketone
MO	Mesityl oxide
SEM	Scanning electron microscopy
S_{MIBK}	Selectivity towards methyl isobutyl ketone
TEM	Transmission electron microscopy
X_{Ac}	Acetone conversion
Y_{MIBK}	Yield towards methyl isobutyl ketone

APPENDICES

Appendix 1: Determination of the acid capacity

The acid capacity of the prepared catalyst was determined before and after its catalytic activity test, by titration. The determination of the acid capacity of the ion exchange resins, can be divided in two different parts, the standardization of the solutions and the titration of the ion exchange resin. The procedure used to standardize the different solutions is shown below:

- 1) First of all, a 0.1 M potassium hydrogen phthalate (KHP) solution was prepared.
- 2) Then, the preparation of a 0.1 M sodium hydroxide solution was carried out. This solution was standardized with KHP using phenolphthalein as indicator.
- 3) A 0.1 M hydrochloric acid solution was provided by Thermo Fisher Scientific. It was standardized with NaOH using methyl orange as indicator.

Once the solutions were prepared and standardized, it was possible to move on to the determination of the acid capacity. Its procedure is listed below:

- 1) Between 1 and 2 grams of the dried ion exchange resin was weighted and introduced to a 150 mL beaker.
- 2) Then, 150 mL of the standardized 0.1 M NaOH solution and 50 mL of a 2.5 wt.% NaCl solution were added to the beaker.
- 3) The mixture was then stirred for 24 hours.
- 4) A 25 mL aliquot was then titrated with the standardized HCl solution, using methyl orange as indicator. This step was repeated, at least, three times.
- 5) The acid capacity is then determined with equation 1, which is shown below:

$$\left[H^+ \right] = \frac{150\text{mL} \cdot C_{NaOH} - (V_{HCl} \cdot C_{HCl}) \cdot \frac{200\text{mL}}{V_{\text{aliquot}}}}{m_{\text{cat}}} \quad (1)$$

Where H^+ is the acid capacity expressed as meqH^+/g , C_{NaOH} and C_{HCl} refers to the concentration of the NaOH and HCl solutions expressed as mol/L , V_{HCl} is the volume of the HCl solution that has been used in the titration expressed in mL, V_{aliquot} is the aliquot volume expressed in mL while m_{cat} stands for the ion exchange resin mass expressed in grams.

Appendix 2: Chromatographic response

Table 9. Retention time of the different species

Compound	Water	Acetone	MIBK	MO
Retention time [min]	3.2	3.4	4.5	5.0

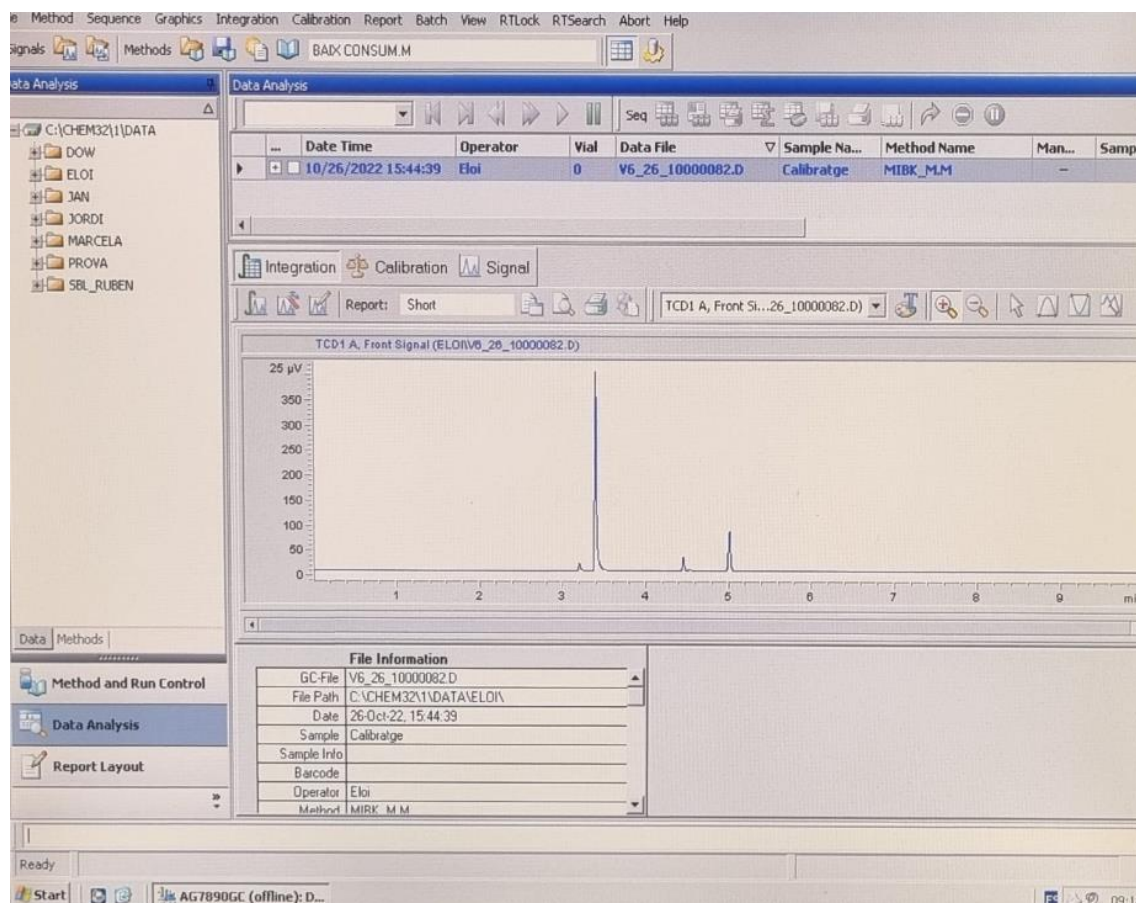


Figure 14. Chromatographic response of the different species.

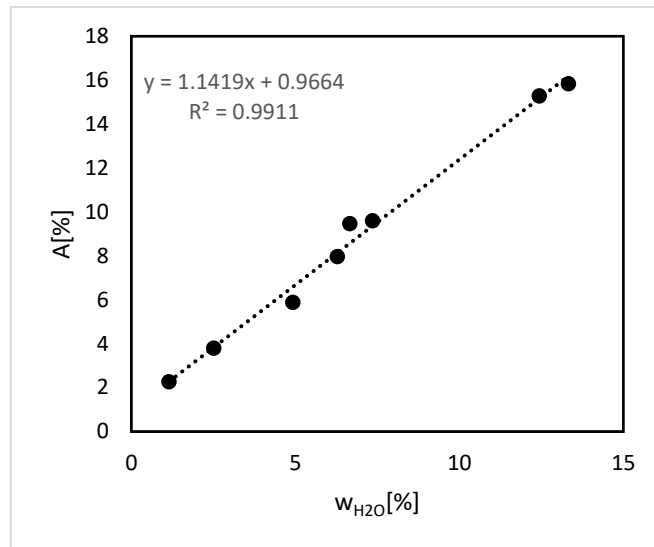
Appendix 3: Graphical representation of the calibration equations

Figure 15. Water calibration equation

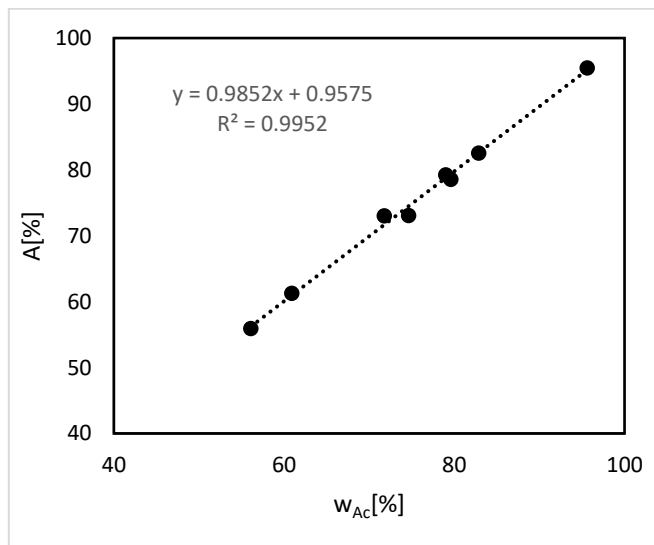


Figure 16. Acetone calibration equation

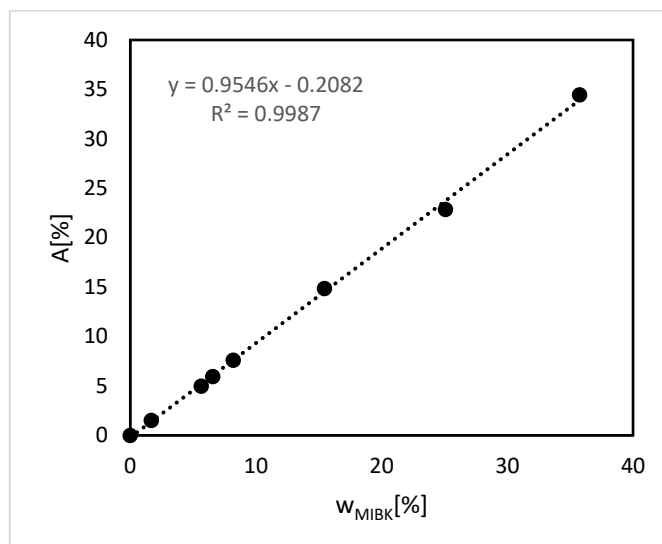


Figure 17. MIBK calibration equation

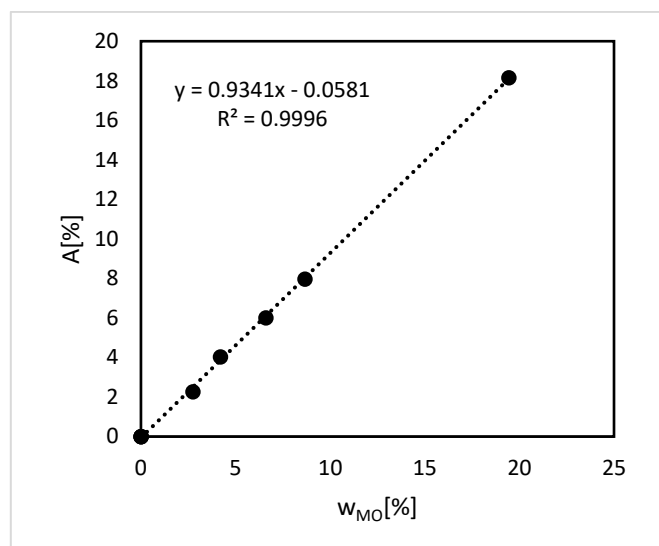


Figure 18. MO calibration equation

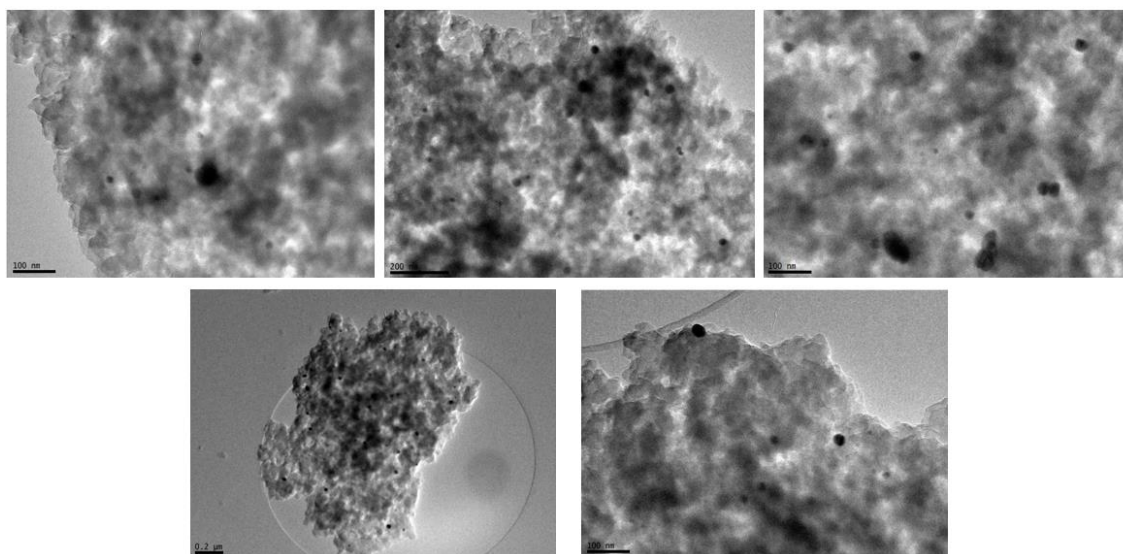
Appendix 4: TEM images of the tested catalysts

Figure 19. TEM images of the A15-1%Pd before the catalytic activity test

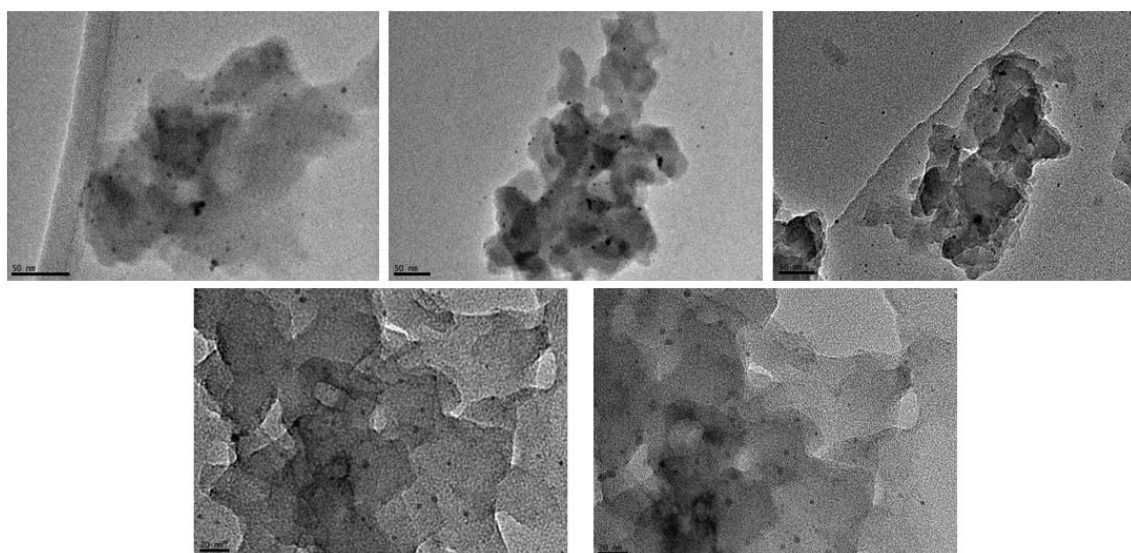


Figure 20. TEM images of the A15-1%Pd after the catalytic activity test

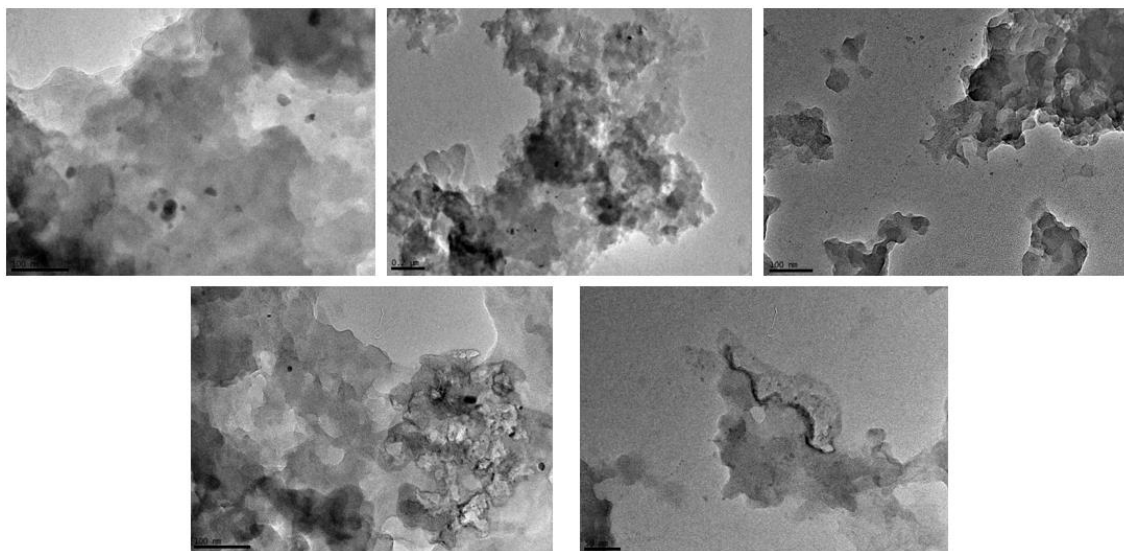


Figure 21. TEM images of the A15-1%Cu before the catalytic activity test

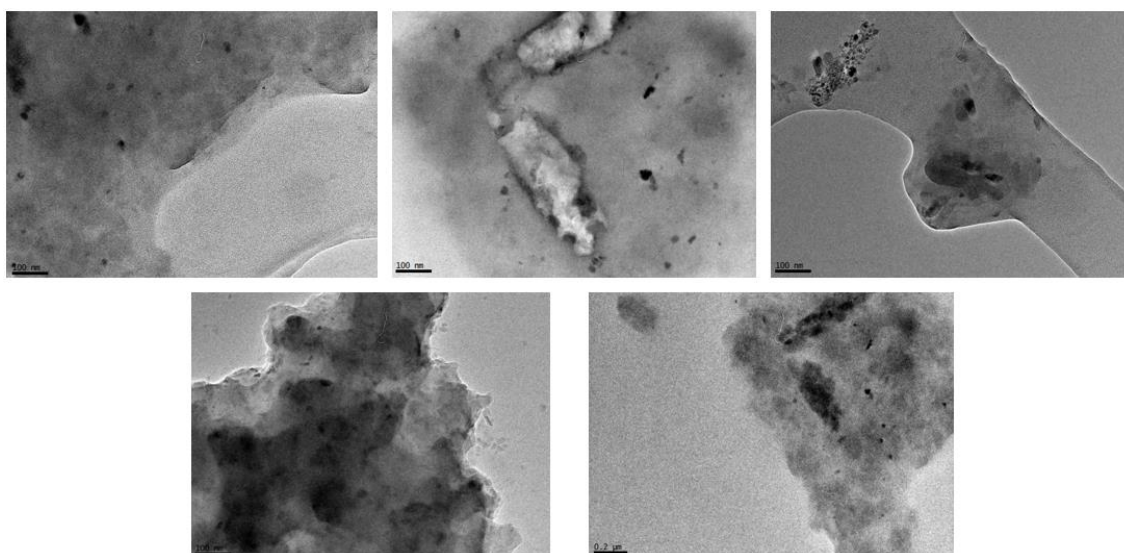


Figure 22. TEM images of the A15-1%Cu after the catalytic activity test

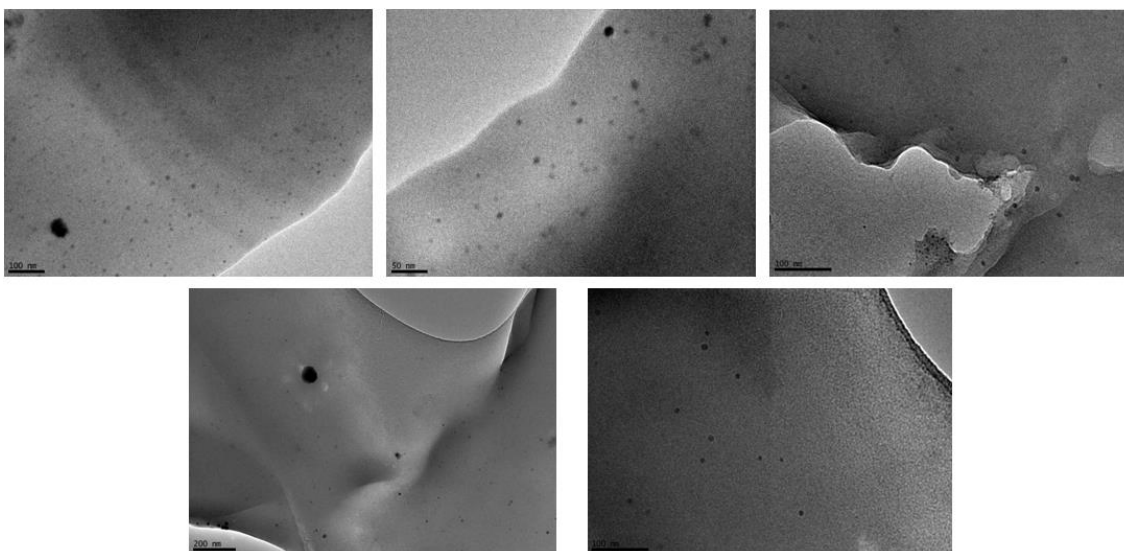


Figure 23. TEM images of the Dow2-1%Pd before the catalytic activity test

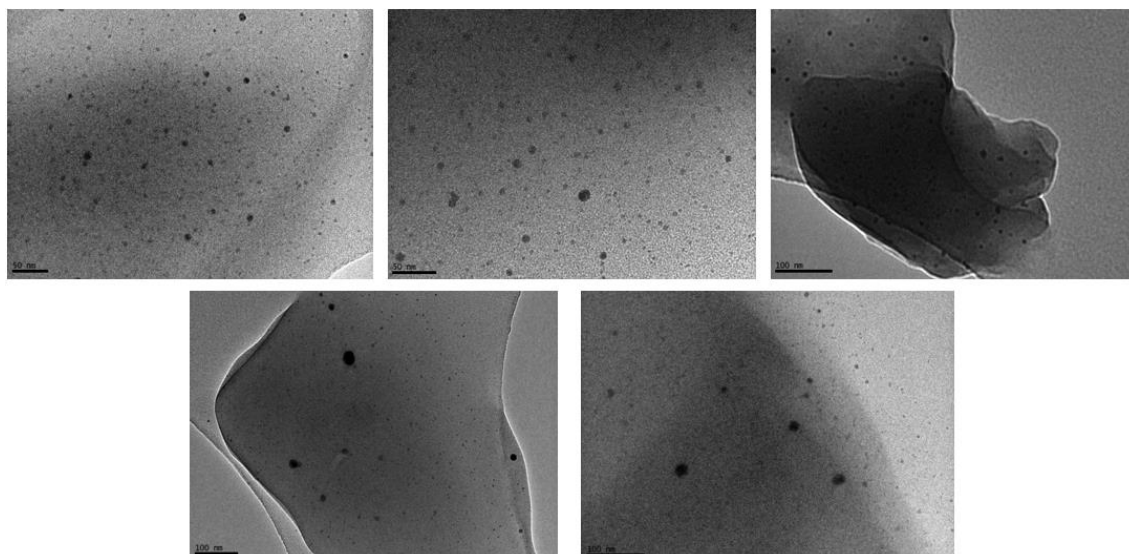


Figure 24. TEM images of the Dow2-1%Pd after the catalytic activity test

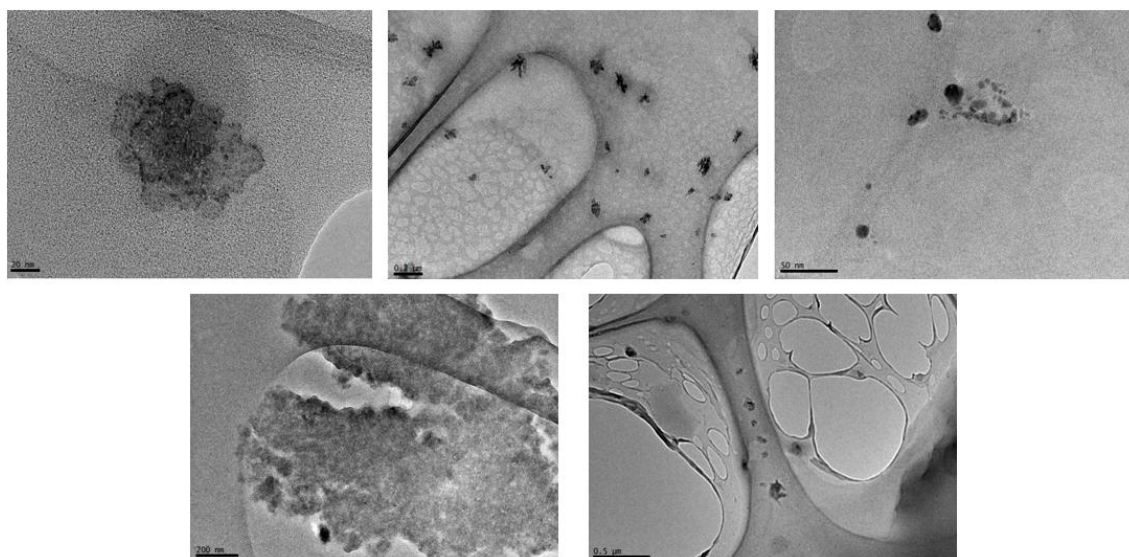


Figure 25. TEM images of the Dow2-1%Cu before the catalytic activity test

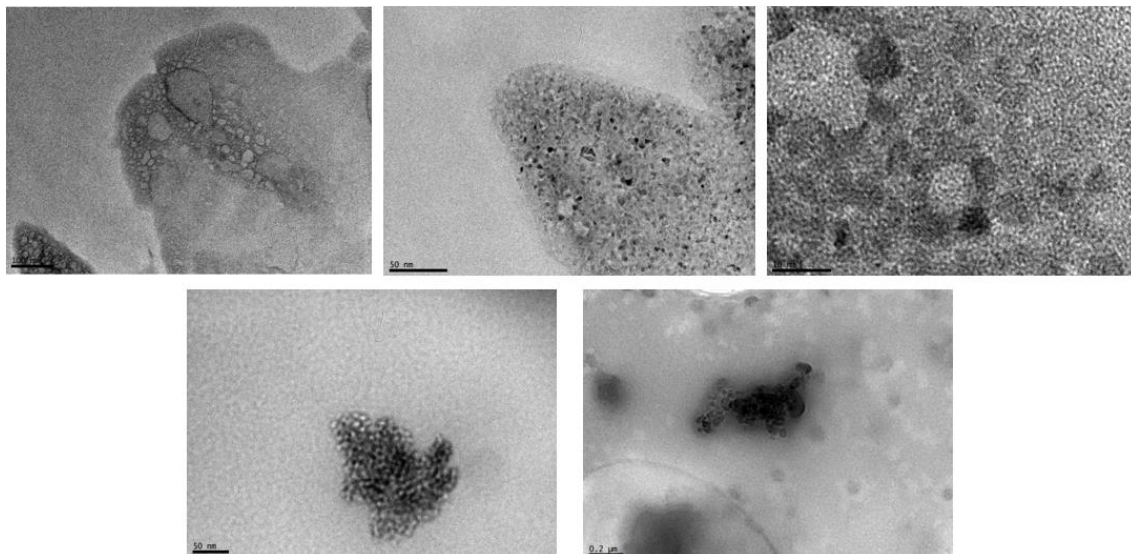


Figure 26. TEM images of the Dow2-1%Cu after the catalytic activity test

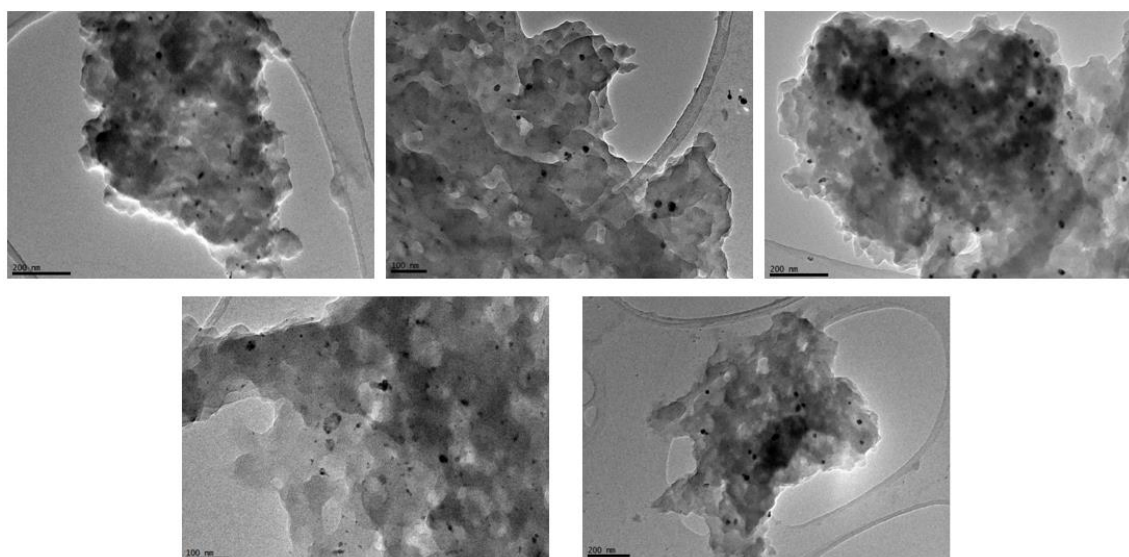


Figure 27. TEM images of the CH28 after the catalytic activity test

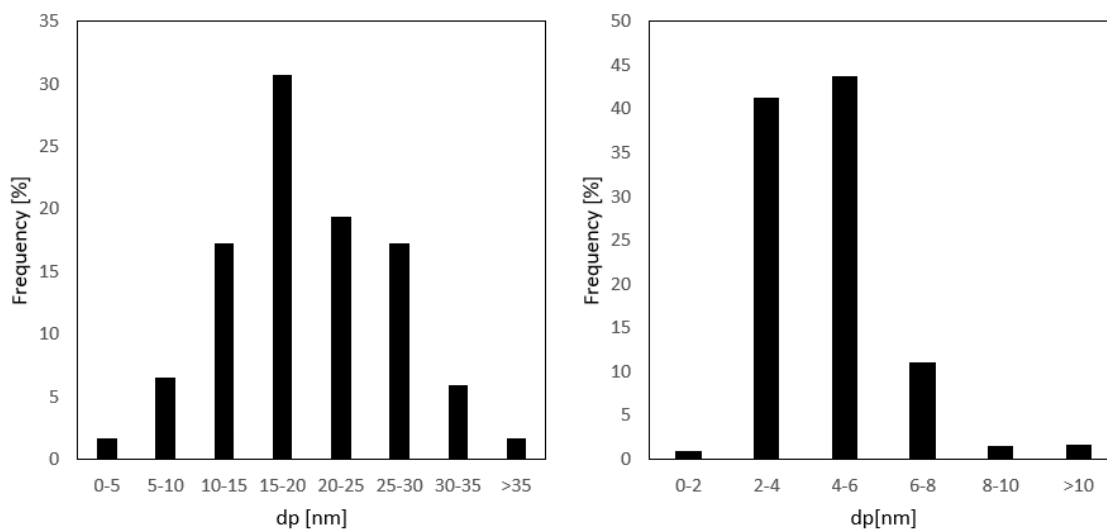
Appendix 5: Metal size distributions of the tested catalysts

Figure 28. A15-1%Pd before (left) and after (right) the catalytic activity test

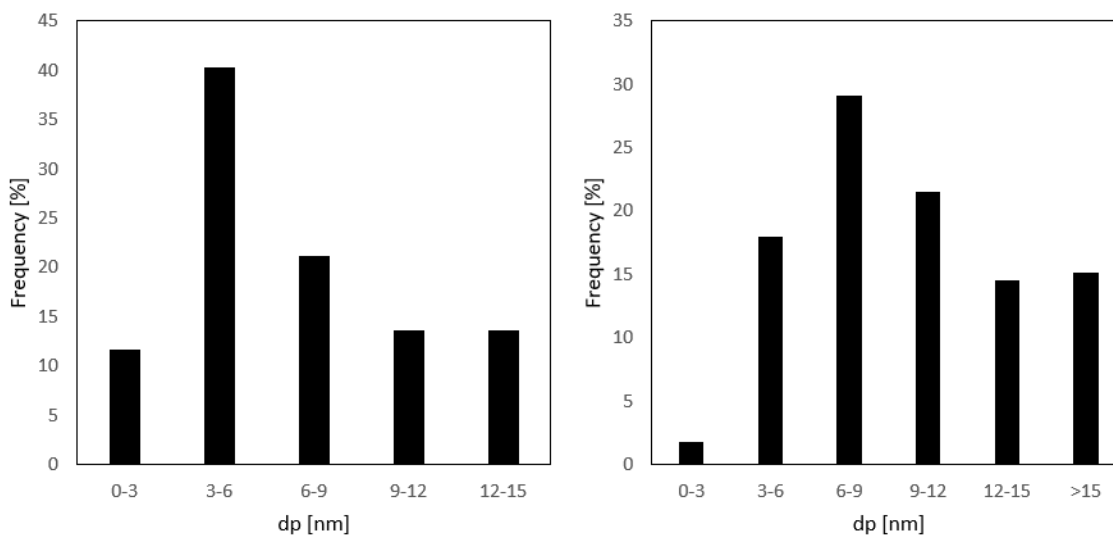


Figure 29. A15-1%Cu before (left) and after (right) the catalytic activity test

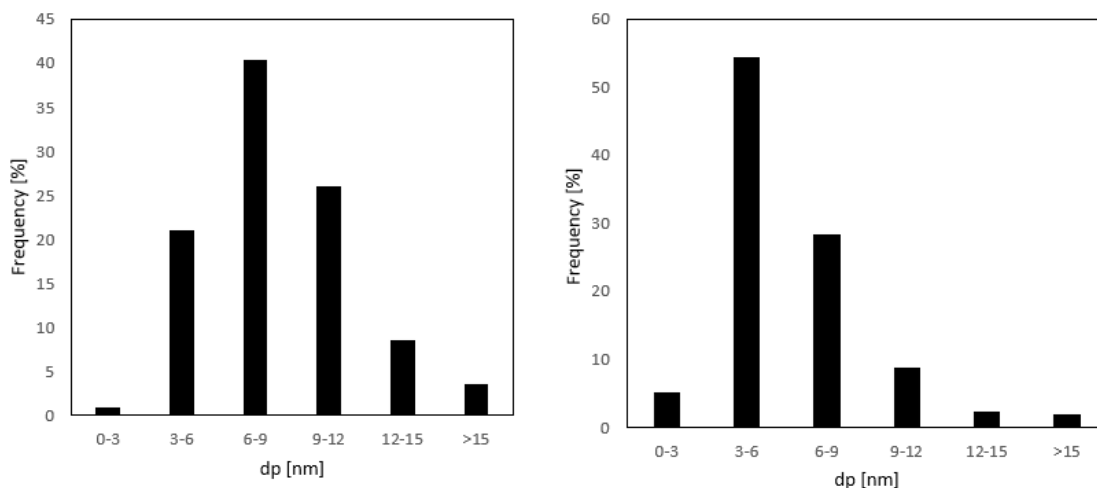


Figure 30. Dow2-1%Pd before (left) and after (right) the catalytic activity test.

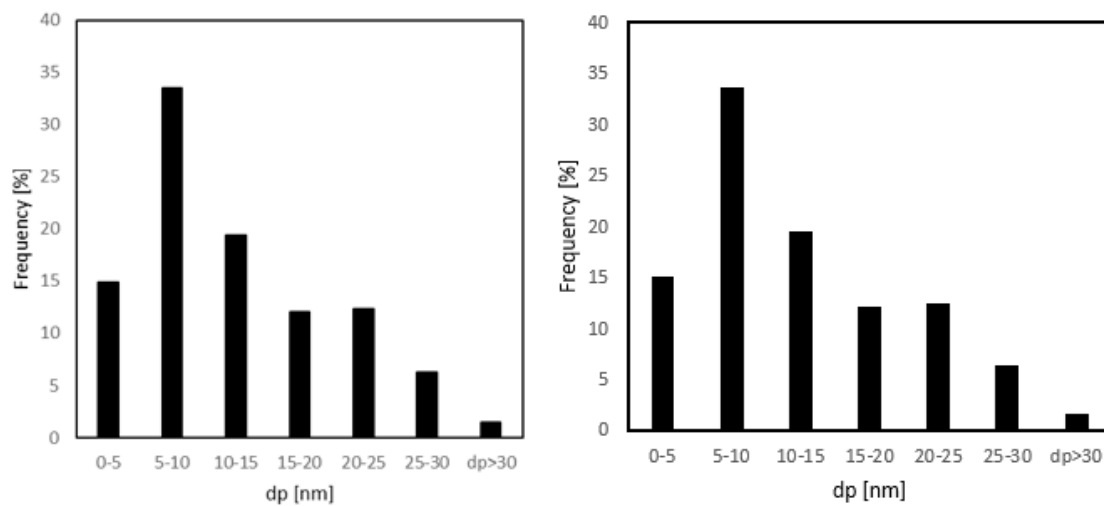


Figure 31. ACH28 before (left) and after (right) the catalytic activity test

Appendix 6: SEM images of the prepared catalysts

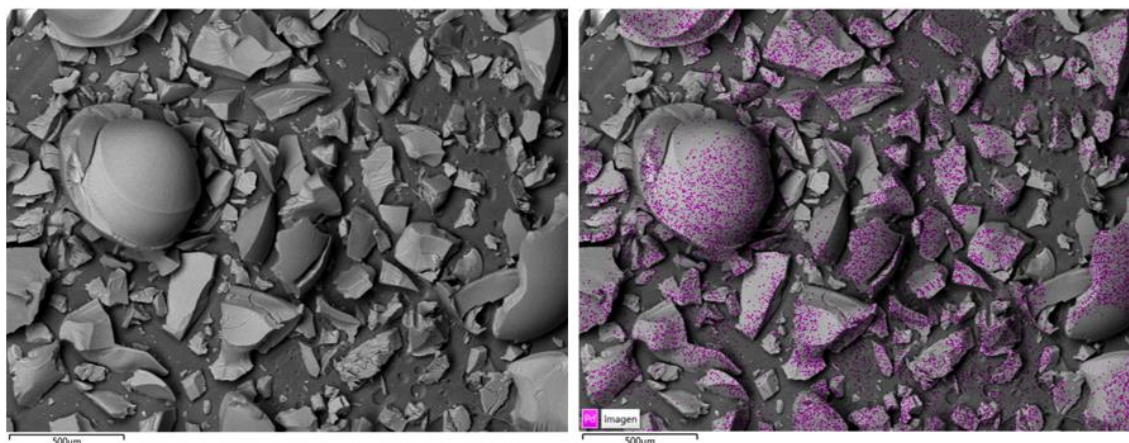


Figure 32. Fresh A15-1%Pd

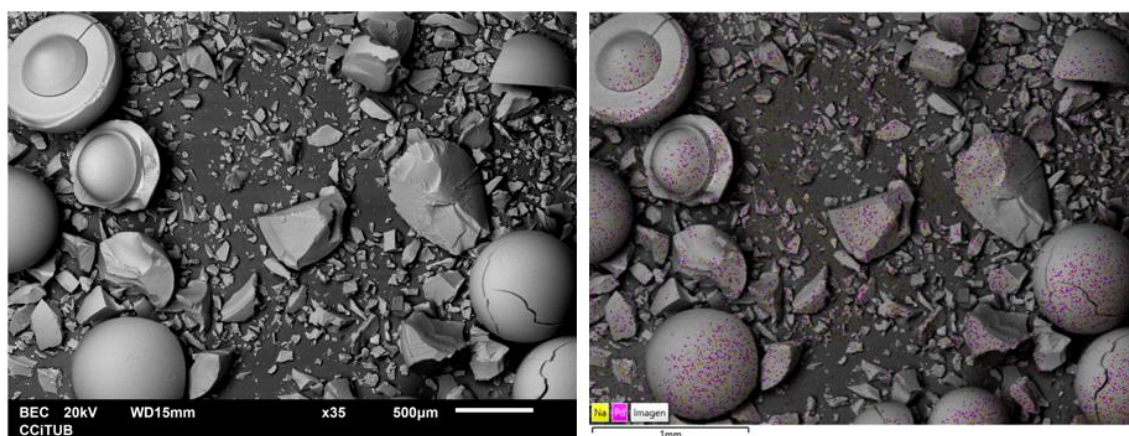


Figure 33. Used A15-1%Pd

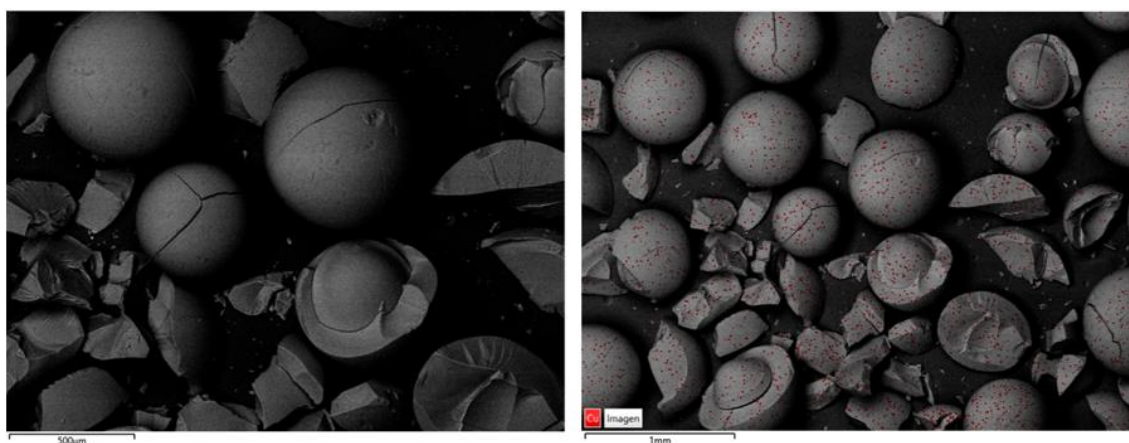


Figure 34. Fresh A15-1%Cu

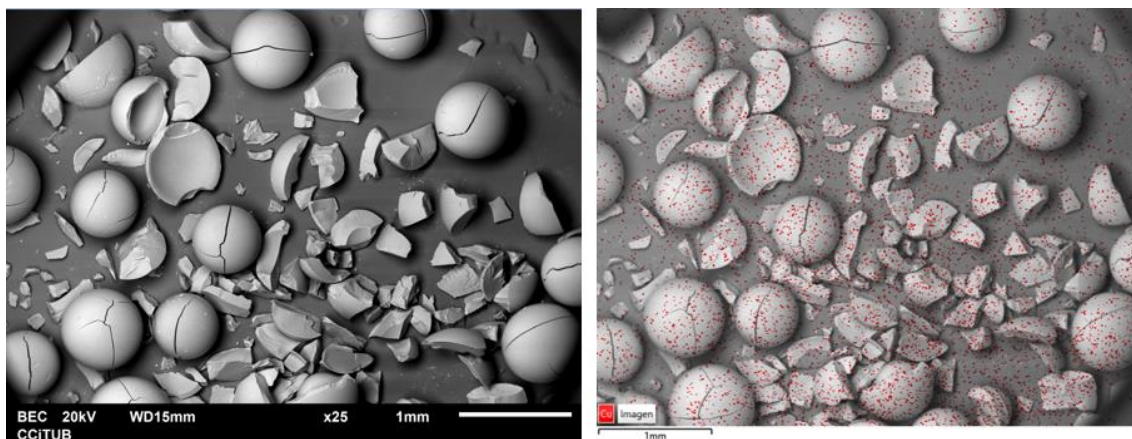


Figure 35. Used A15-1%Cu

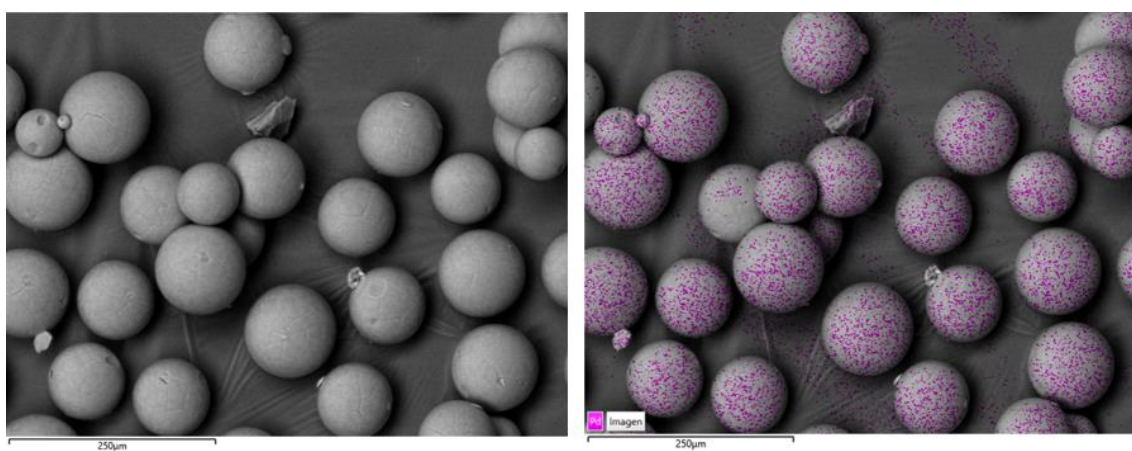


Figure 36. Fresh Dow2-1%Pd

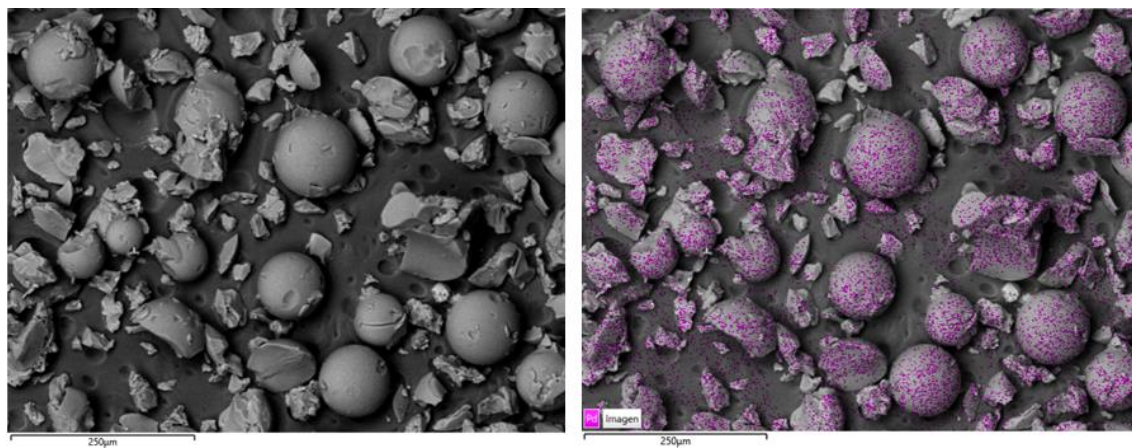


Figure 37. Used Dow2-1%Pd

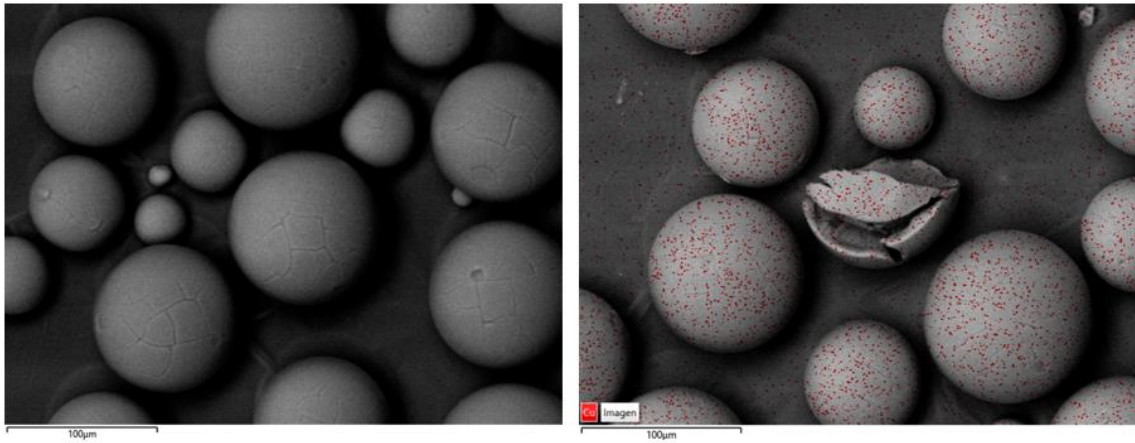


Figure 38. Fresh Dow2-1%Cu

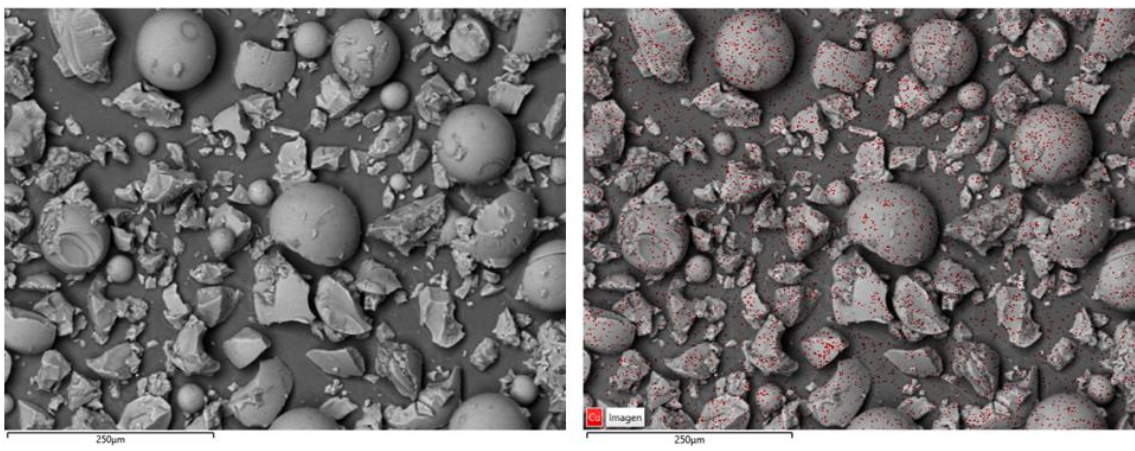


Figure 39. Used Dow2-1%Cu

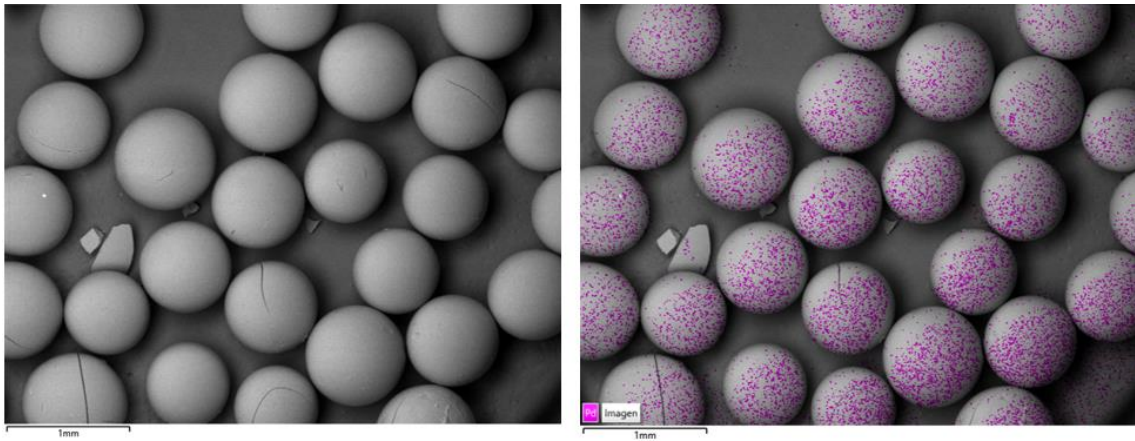


Figure 40. Used ACH28